Cdk1 has a role in phosphorylating TRAMM

Sari Snounou

A Thesis
in
The Department
of
Biology

Presented in Partial Fulfillment of the Requirements

for the Degree of Master of Science (Biology) at

Concordia University

Montreal, Quebec, Canada

September 2017

CONCORDIA UNIVERSITY
School of Graduate Studies

This is to certify that the thesis prepared

By: Sari Snounou

Entitled: Cdk1 has a role in phosphorylating TRAMM

and submitted in partial fulfillment of the requirements for the degree of
Master of Science (Biology)
complies with the regulations of the University and meets the accepted standards with respect to originality and quality.
Signed by the final Examining Committee:

_____Chair
To be Determined

_____Examiner
Dr. A. Piekny

_____Examiner
Dr. W. Zerges

_____Examiner
Dr. V. Titorenko

_____Supervisor
Dr. M. Sacher

Approved by _____
Dr. G. Brown (Graduate Program Director)

_____2017 _____
Dr. A. Roy (Dean of Faculty of Arts and Science)

ABSTRACT

Cdk1 has a role in phosphorylating TRAMM

Sari Snounou

TRAMM was originally identified as a protein that co-precipitates with the TRAPP (transport protein particle) complex that functions in membrane trafficking. Recent work in our laboratory suggested a role for this protein in mitosis, specifically in chromosome congression prior to metaphase. In the early stages of mitosis, TRAMM is post-translationally modified by phosphorylation. Knockdown of the protein causes it to affect the localization of various kinetochore proteins with the strongest effect on CENP-E. The two proteins were also shown to interact using a yeast two hybrid assay (Milev et al., 2015).

In this study, I show that TRAMM also interacts with CENP-E through a co-immunoprecipitaiton assay and this interaction appears to be enhanced in mitotic lysates. Using various inhibitors of mitotic kinases, I further show that only inhibition of Cdk1 prevents the phosphorylation of TRAMM. This suggests that Cdk1, apart from the other mitotic kinases, has a role in phosphorylating TRAMM. Furthermore, I also use bioinformatics tools to predict the structure of TRAMM. Finally I express and purify a recombinant form of TRAMM in a homogeneous monodispersed protein sample.

ACKNOWLEDGEMENTS

I would like to thank my supervisor Dr. Michael Sacher for his passions, patience, guidance and mentoring during my study. In a 2-year period I had the chance to learn a lot from Dr. Sacher not only in biology. I have learned from him invaluable skills including critical thinking as well as working in a team efficiently. I would also like to thank my committee members Dr. Alisa Piekny and Dr. Vladimir Titorenko for their helpful suggestions.

Thank you to my colleagues and friends at Concordia for helping me with my research. I would like to especially thank Miroslav, Stephanie, Djenann, Daniela, Keshika, Rodney, Benedeta for all their invaluable help.

I would also like to thank the laboratory of Dr. Kornblatt, who performed the dynamic light scattering analysis and the laboratory of Alain Tessier who performed the mass spectrometry.

Finally, I would like to thank my family Hiyam, Salim, Issam, Louay unconditionally.

I am also grateful for the financial supports I received from Concordia University.

TABLE OF CONTENTS

LIST OF FIGURES

LIST OF TABLES

Chapter 1: Introduction

1.1 Membrane trafficking

Membrane trafficking is an essential cellular process that occurs in virtually every cell. This process allows the cell to specifically deliver cargo molecules between its organelles, as well as their secretion to the extracellular space through exocytosis. This process is mediated by transport vesicles. The appropriate targeting of a vesicle requires a series of molecular events including sorting, budding, movement, tethering, and fusion of the vesicle. Each step increases the specificity of the trafficking process (Bonifacino and Glick, 2004). An example of this would be Endoplasmic Reticulum (ER) to Golgi traffic, where proteins are properly folded and packaged into coated vesicles (COPII), and transported from the ER to the Golgi (Hughes and Stephens 2008). In the Golgi, proteins are subjected to post translational modifications such as glycosylation, phosphorylation and packaging into carrier vesicles that bud from the trans-Golgi, allowing them to be transported to other cellular locations (Godi et al., 2004).

1.1.1 TRAPP complex

In 1998, Sacher and colleagues described the transport protein particle (TRAPP) complex while working on a protein called Bet3 (a 22KDa hydrophilic protein involved in ER-Golgi transport) (Sacher et al., 1998).Through epitope tagging of Bet3p and its purification from cell lysates in *Saccharomyces cerevisiae*, Bet3p was found to be a member of a large complex that is now known as TRAPP. This complex is specifically involved in the tethering process, as it is the first contact between vesicles and their target membrane. The TRAPP complex is considered to be one of the best studied of the multisubunit tethering complexes at the molecular level (Sacher et al., 2008).

TRAPP I, II and III are three forms of TRAPP that were found to co-exist in *S. cerevisiae*. Studies show that all TRAPP complexes share the function of being a guanine nucleotide exchange factor (GEF) for Ypt1. This is accomplished by conserving 4 of their typical 6 core subunits: Bet3p, Bet5p, Trs23p, and Trs31p (Kim et al., 2006). These conserved subunits along with two additional subunits (Trs33p and Trs20p) form the TRAPP I complex. This complex functions at the level of ER-to-Golgi trafficking by

binding to COPII-coated ER-derived vesicles, and brings them to closer proximity of the acceptor membranes (Sacher et al., 1998). TRAPP II is composed of 10 subunits (the TRAPP I subunits and an additional 4 subunits; Trs65p, Trs120p, Trs130p and Tca17p) found to function at the level of intra-Golgi and late Golgi trafficking (Sacher et al., 2001). TRAPP III is made up of 7 subunits (the six TRAPP I subunits and an additional subunit called Trs85p) and functions in selective and non-selective autophagy (Lynch-Day et al., 2010).

The TRAPP complex is conserved throughout eukaryotes. It is found in mammals in an organized fashion represented by TRAPP II (consisting of C1, C2, C2L, C3, C4, C5, C6, C9, and C10) and TRAPP III (C1, C2, C2L, C3, C4, C5, C6, C8, C11, C12, C13) (Zong et al., 2011). This includes mammalian orthologues and additional unique mammalian subunits such as TRAMM (previously called TRAPPC12) and TRAPPC13 (also known as FLJ13611) (Table 1.1) (Sacher and Milev, 2016).TRAPP II and TRAPP III share the basic core subunits. What differentiates them are the C9 and C10 subunits in TRAPP II while TRAPP III contains C8, C11, C12, and C13 (Bassik et al., 2013). The TRAPP complex function is partially conserved since the mammalian TRAPP II complex is a GEF for Rab1 (Rab1 is an orthologue to yeast Ypt1p) (Ishikawa et al., 2009). The mammalian TRAPP III complex is functionally similar to that of yeast as it is involved in cellular autophagy (Behrends et al., 2010).

1.1.2 TRAMM

Trafficking of membranes and mitosis (TRAMM) is a 79 KDa protein that is one of the subunits of the mammalian TRAPP III complex (Scrivens et al., 2011). Depletion of TRAMM in HeLa cells results in Golgi fragmentation suggesting that it functions at an early stage of ER-to-Golgi trafficking (Scrivens et al. 2011). Interestingly, a recent discovery in our laboratory has shown that TRAMM has an important function in mitosis. TRAMM is the only subunit of TRAPP complex that has a role in mitosis (Figure 1.1(A)). Upon depletion of TRAMM, some chromosomes failed to congress to the metaphase plate and the cells remained arrested in this pre-metaphasestate of mitosis (Figure 1.1(C)). TRAMM is phosphorylated during early mitosis (Figure 1.1(B)) and this phosphorylation plays a critical role in CENP-E recruitment to the kinetochores (see below) (Milev et al., 2015).

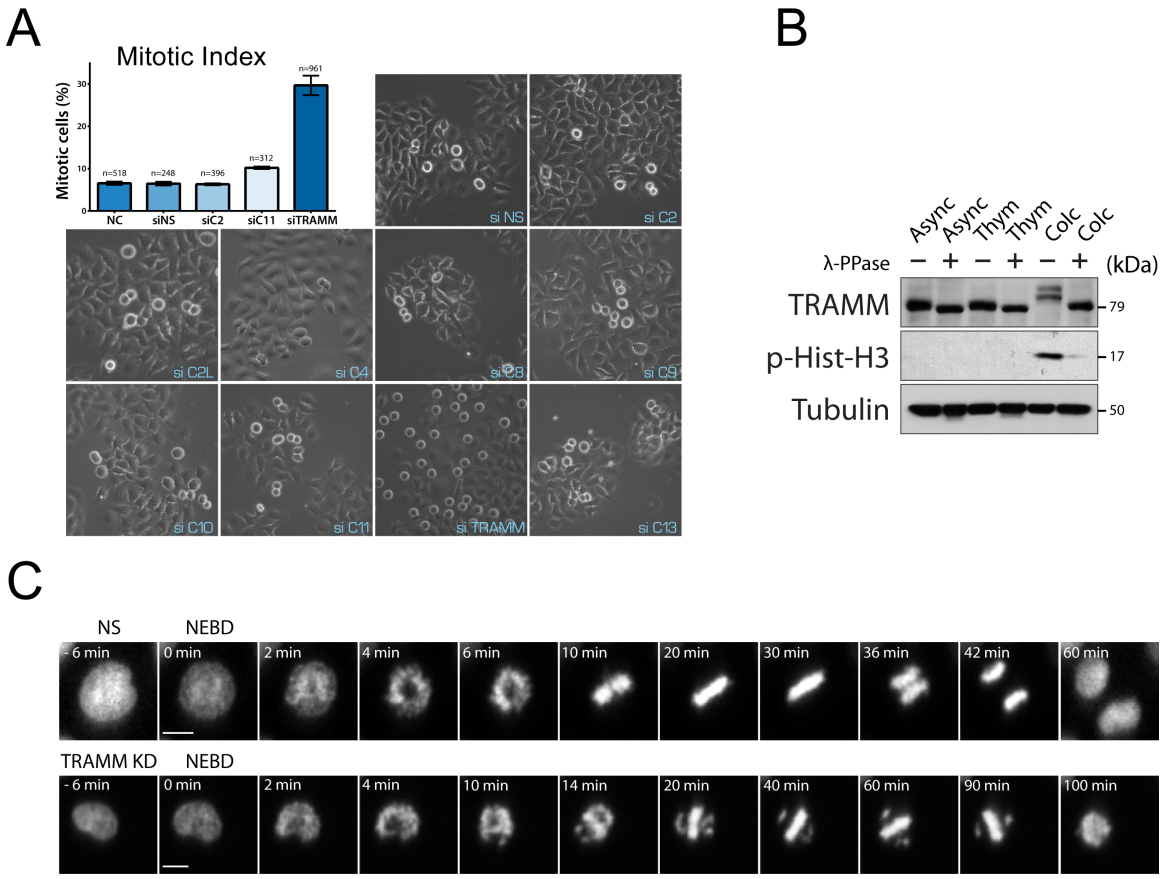

Figure 1.1 TRAMM has a role in mitosis. (A) Hela cells were photographed by bright field microscopy 24h after treatment with siRNA against the TRAPP subunits indicated. Cells were quantified by counting the number of mitotic cells in multiple fields. Depletion of TRAMM arrested cells in mitosis. Quantification of this effect indicated that the mitotic index increased from 6.4% for untreated (NC) or nonspecific siRNA (siNS) to 29.7% after depletion of TRAMM. This effect was not seen for other subunits of TRAPP complex indicating that TRAMM is the only subunit of TRAPP that has a role in mitosis. (B) Western blots of Hela cell lysates probed for anti-TRAMM, anti-phospho histone-H3 (p-Hist-H3) (mitotic marker) and anti-tubulin (loading control). Hela cells were leftuntreated (asynchronous), treated with thymidine to arrest the cells at G1/S (Thym), or treated with colcemid (colc) to arrest the cells in mitosis. Colcemid treatment of cells reduced the mobility of TRAMM from 79 KDa (in asynchronous cells and thymidine-treated cells) to 83 KDa. Phosphatase treatment increased the mobility of colcemid-treated cells from 83 KDa to 79 KDa indicating that TRAMM is mitotically

phosphorylated. (C) Hela cells expressing fluorescently labeled histone H2B were treated with non-specific (NS top row) or TRAMM (bottom row) siRNA. The cells were subjected to live cell imaging 20 hours after treatment. Time at 0min refers to nuclear envelope break down in prophase (NEBD). TRAMM knockdown (KD) led to the presence of polar chromosomes that never migrated to the metaphase plate indicating that TRAMM has a role in chromosome congression (Milev et al., 2015).

1.1.3 Membrane trafficking proteins in mitosis

Proteins with at least two unrelated functions are described by the term “moonlighting.” Studies have shown that many membrane trafficking proteins have “moonlighting” functions in mitosis. TRAMM is one amongst the many such as clathrin, dynamin, epsin, and cyclin-G associated kinases (GAKs) (Royle, 2012).

Clathrin is a protein coat used by cells to assist in the budding of vesicles from their respective donor membranes (Maro et al., 1985). Clathrin is also found in mitotic spindles, and its depletion destabilizes kinetochore fibers even though they are entirely lacking membranes (Royle et al., 2005). GAK is an auxillin homologue that is a threonine and serine kinase that is associated with cyclin-G and functions in the removal of clathrin from clathrin coated vesicles. Interestingly, the depletion of GAK resulted in cellular arrest in pre-metaphase, showing mitotic moonlighting functionality (Greener et al., 2000).

1.2 Mitosis

Mitosis starts with chromosome condensation and ends with two daughter cells that have identical numbers of chromosomes. This process comprises 5 phases: prophase, prometaphase, metaphase, anaphase, and telophase (De Souza and Osmani, 2007).

During prophase, the chromosomes begin to condense and are held together in pairs by the action of cohesion complexes. This is followed by nuclear breakdown (in most eukaryotes) and centrosomes begin to move towards opposite poles of the cell (Howell et al., 2001). The Knl1-Mis12 -Ndc80 (KMN) complex becomes active to bind to the

kinetochores at the centromeres of the condensed chromosomes and spindle microtubules start to appear from centrosomes in preparation for prometaphase (see below) (Muller-Reichert et al., 2007). Microtubule elongation and attachment to the kinetochores, and further chromosomal condensation for the purpose of alignment at the metaphase plate occur during prometaphase (May and Hardwick, 2006). The movement of chromosomes to the metaphase plate at the center of the cell is known as chromosome congression and upon completion of this process the cells are said to be in metaphase (May and Hardwick, 2006). Anaphase corresponds to the movement of the sister chromatids to opposite poles of the cell via microtubule depolymerization. The last phase of mitosis is telophase, where the nuclear membrane reforms, nuclei reappear, chromosomes decondense to chromatin, and the remaining spindle microtubules depolymerize (Bucciarelli et al., 2003). Concurrently with telophase, cytokinesis forms actin-myosin rings in the center of the cell, which results in cellular abscission to create two identical daughter cells post mitosis (Lara-Gonzalez et al., 2012).

1.3 Kinetochores

Kinetochores (KT) are inner proteinaceous complexes (greater than 200 proteins in mammalian cells) that assemble on the centromere of each chromosome (Errico et al., 2010). KTs mediate the interactions between the centromere of sister chromatids and spindle microtubules (MTs), mediating all movements of chromosomes during mitosis (O'Connor et al., 2008). They have been conserved throughout eukaryotes due to their evolutionary importance in mitosis and are composed of two main core components: the Constitutive Centromere-Associated Network (CCAN) and Knl1-Mis12 -Ndc80 (KMN) complex network (Godek et al., 2015).

CCAN are part of the inner portion of KTs that directly bind to the centromeric nucleosomes and links them to the KMN network. This is possible due to CCAN's histone H3 variant known as CENP-A, which is a component of a larger 16 centromeric protein complex (Figure 1.1) (Musacchio and Salmon, 2007).

The KMN network is located on the outer portion and is responsible for the interaction with kinetochore microtubules (the binding of KTs to MTs) and serves as a spindle assembly checkpoint (SAC) protein scaffold (Musacchio et al., 2011). The outer KT only

assembles post-NEBD and consists of approximately 20 proteins (mostly microtubule interacting proteins) adjacent to the CCAN. These outer KT proteins include KMN, mitotic checkpoint proteins, and motor proteins including CENP-E (see below) (Musacchio and Salmon, 2007). The KMN network, consisting of 3 major components (Knl1, Mis12 and Ndc80 complex) associates with KTs.

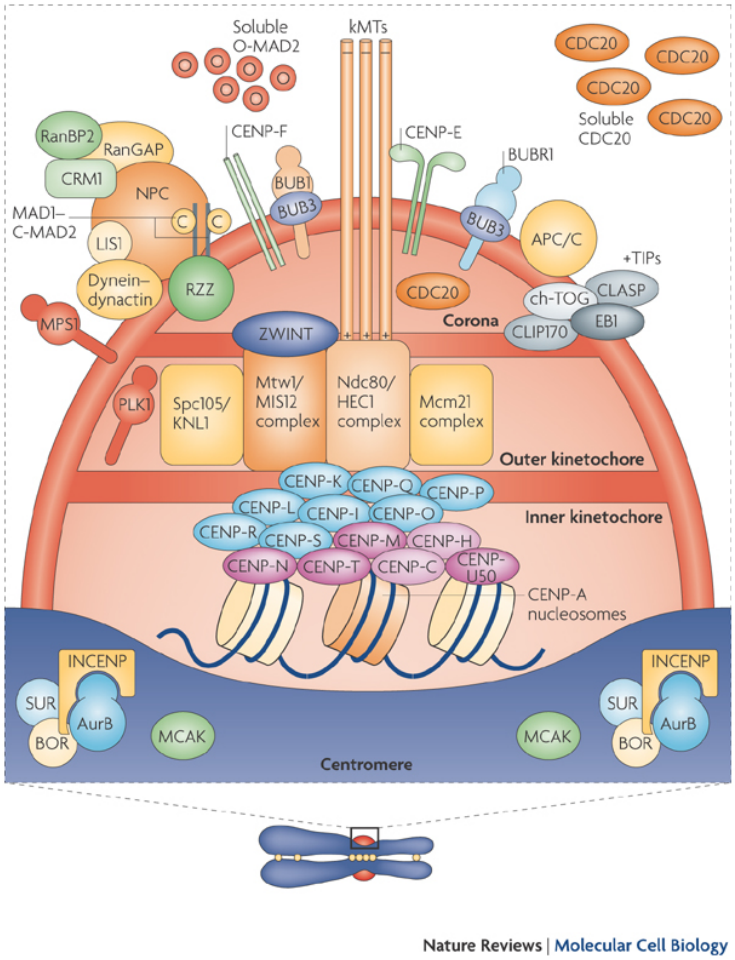

Nature Reviews | Molecular Cell Biology

Figure 1.2 Kinetochore Structure at the Centromere. This cross-sectional view of the kinetochores show its complex macro structure consisting of many protein complexes. These complexes include the CENP-A protein complex (consisting of 16 centromere proteins), KMN network, SAC, CPC, APC, INCENP, etc. Microtubule attachment is present at the KMN network. This structure represents post nuclear envelope breakdown (NEBD) due to CENP-E binding to MT. SAC seems to be inactive in this representation due to the soluble Cdc20 available to activate APC. Although Mad1:Mad2 complex is present, there are no interactions with open Mad2 and no presence of Mad2:Cdc20 complex. Overall this shows a state of mitotic progression around metaphase of Mitosis.

(Musacchio and Salmon, 2007)

The outer kinetochore assembly and recruitment is performed by the Mis12 complex, as it recruits Knl1 that further draws the centromere and spindle assembly checkpoint (SAC) proteins into proximity (Cheeseman et al., 2008). The Ndc80 complex increases the binding affinity of KT to the MT via electrostatic interactions with the aid of Mis12 and Knl1 (Cheeseman et al., 2008). The Ndc80 complex also interacts with the spindle- and kinetochore-associated (Ska) complex, which is required for anaphase transition and onset (Errico et al., 2010). Unstable attachments of sister chromatids to the spindle microtubules can activate signaling of spindle checkpoints causing mitotic arrest (Sivakumar et al., 2016). The binding affinity of the KT to the MT can be regulated by phosphorylating the proteins in the KMN network by Aurora B kinase (see below). These mechanisms reduce the possibility of chromosome segregation defects (Cheeseman et al., 2008).

1.4 Mitotic Kinases

Protein phosphorylation is a common process for cellular regulation and cell signaling. Cellular regulation allows for check point control during complex cellular processes such as switching through all the different phases of the cell cycle. Some of the most critical kinases that control the progression of mitosis in the cell cycle are cyclin-dependent kinases (CDKs), Polo-like kinases (Plks), and Aurora Kinases (Santamaría et al., 2007).

1.4.1 Cyclin-dependent Kinases

Mammalian cell cycle progression is highly dependent on the activity of CDKs due to their regulatory impact by phosphorylating key substrates (Santamaría et al., 2007). The concentrations of CDKs are relatively constant during the cell cycle, but the activity of this family of enzymes is highly dependent upon the expression levels of cyclins in the cell, and they are only active in their cyclin-CDK complex. Due to the variable expression of cyclins and their specificity towards binding CDKs (as each CDK can bind to a specific cyclin), they can be used as biomarkers during all stages of the cell cycle (Satyanarayana and Kaldis, 2009). The transition between phases of the cell cycle is

driven by the changing concentration of cyclins within the cell as cellular arrest occurs if an issue arises with production or degradation of these substrates (Malumbres and Barbacid, 2009).

1.4.2 Cyclin-dependent Kinase 1

Cdk1 is highly regulated as it functions in the irreversible transition of the cell from Interphase to mitosis. Due to the critical role of Cdk1 in this process, it is regulated through compartmental barriers, phosphorylation (at threonine 14 and tyrosine 15), and by the presence of Cyclin A and B (which can also be regulated through phosphorylation) (Potapova et al., 2009). Cyclin A remains associated with Cdk1 from late S into late G2-phase. The increase in cyclin B concentrations in the cytoplasm pushes the formation of cyclin B-Cdk1 complex leaving free cyclin A, which is degraded by ubiquitination(Fung et al., 2005). This event initiates prophase as more cyclin B-Cdk1 complexes form. The complexes remain inactive as ATP orientation within the active site of the kinase is altered because the threonine 14 and tyrosine 15 residues have been phosphorylated by Wee and Myt kinases (Potapovaet al., 2009). The cyclin B-Cdk1 complex is only in its active form after Cdc25 phosphatase dephosphorylates these two residues (Mailand et al., 2002). Cdc25 is regulated by phosphorylation via Polo-like kinases (Plks) (see below) as a further measure of mitotic regulation (Mailandet al., 2002).

Activated cyclin B-Cdk1 is located in the cytoplasm but the nucleus acts as a compartmental barrier, preventing it from phosphorylating its target substrates. Cyclin B-Cdk1 complexes up-regulate their own transport into the nucleus as their overall concentration increases within the cytoplasm (Lindqvist et al., 2010). The entry of the complex may occur slightly before NEBD (Gavet and Pines 2010). Once in the nucleus, signal cascades result in spindle stabilization and elongation. Cyclin B-Cdk1 also increases expression of survivin and other key substrates that are critical for mitotic progression (Lindqvist et al., 2010). Knockdown of cyclin B, Cdk1 or cyclin B-Cdk1 complex can result in cellular arrest or apoptosis due to low survivin levels, as well as cells having difficulty polarizing causing mitotic disarray (Castedo et al., 2002). Mitosis initiates with cyclin B-Cdk1 complex and the degradation of cyclin B at anaphase triggers mitotic exit (Errico et al., 2010).

1.4.3 Aurora and Polo-like kinases

Polo-like kinases (Plks) are enzymes that play important roles in mitotic entry, exit, and spindle formation. They are shown to have high expression during mitosis and improper inhibition of this family of enzymes can lead to cellular apoptosis (Wang et al., 2002). Plks are characterized by highly conserved N-terminal serine/threonine kinase domains and polo-box domains (PBDs) at the C-terminus (Lee et al., 2014). One of the most studied members of the Plk family is Plk1. It participates downstream of mitotic entry due to its regulation of Cdc25 via phosphorylation, which leads to the activation of cyclin B-Cdk1 (Lee et al., 2014). Plk1 has further involvement with mitotic spindles, centrosomes, and kinetochores, which makes it a key enzyme during mitosis (Jones et al., 2003).

The mitotic progression and entry into cytokinesis is regulated by Aurora Kinases, a family of serine/threonine kinases (Fu et al., 2007). Three major Aurora Kinases in mammals are Aurora A, B, and C. Aurora A functions near the centrosomes activating cyclin B-Cdk1 by phosphorylating Cdc25B playing a key role in recruiting proteins responsible for the nucleation of microtubules (Marumoto et al., 2002). Aurora B is a subunit of the chromosomal passenger complex (CPC), which contributes to the progression of mitosis by orchestrating chromosomal alignment, cytokinesis, and the modification of histones (Vader et al., 2006) (Carmenaet al., 2013). Aurora C is shown to be versatile as it behaves like Aurora A during interphase and can compensate for low concentrations of Aurora B by acting as its mimic (Salaün et al., 2008).

1.5 Cell Cycle Checkpoints

Cells that undergo the cell-cycle must proceed in a regulated fashion to conserve the integrity of the genome and to ensure proper cell division. To ensure that each phase of

the cell cycle has gone through completion before initiating the next, the conditions of a cell cycle checkpoint must be met or cellular arrest may occur (Malumbres and Barbacid, 2009). Improper bypass of these checkpoints can be intimately linked to psoriasis, neurocutaneousdisorders, and cancer (Malumbres and Barbacid, 2009).Three major checkpoints control the cell cycle. There are two non-mitotic checkpoints, which include the G1 to S-phase and G2 to M-phase checkpoints. The main mitotic checkpoint is the spindle assembly checkpoint (SAC) (Kastan et al., 2004).

1.5.1 Spindle Assembly Checkpoint

The spindle assembly checkpoint (SAC) is a surveillance mechanism that monitors chromosomes within the cell to ensure their proper segregation during mitosis. The core SAC proteins present in mammals are Mad1, Mad2, BubR1, Bub1, and Cdc20 (MCC complex) (Malmanche et al., 2006). SAC is activated if there are any errors in chromosomal attachment to the spindle apparatus. They have to be specifically attached in the proper orientation with the appropriate tension upon the sister centromeres to the extending microtubules from each spindle pole at the opposite ends of the cell (Lara-Gonzalez et al., 2012). Unattached kinetochores prevent SAC inactivation and recruit open Mad2. Open Mad2 can bind with either Mad1 or Cdc20. The mechanism is believed to involve recruitment of Mad2 to Mad1 resulting in closed Mad2. This complex can interact allosterically with other open Mad2 proteins to increase its binding affinity to Cdc20 forming a closed Mad2-Cdc20 complex. The Mad2-Cdc20 complex inhibits Cdc20's interaction with the anaphase promoting complex APC (Caldas and DeLuca, 2013).

The suppression of APC will inhibit anaphase onset and progression of mitosis. APC functions as a ubiquitin ligase that is responsible for the degradation of cyclin B which arrests the cell in mitosis (see below) (Fung et al., 2005). It also degrades securin resulting in the activation of separase that functions in cleaving the cohesion complex, separating the sister chromatids from each other (Fu et al., 2005). This ubiquitin ligation is mediated by the cofactor Cdc20 (Morgan et al., 2007).

The SAC ensures that misaligned chromatids do not separate. One possible cause for misalignment can be errors in MT-KT capture by CENP-E. If this issue bypasses the

SAC, the daughter cells may have unequal chromosomes (aneuploidy) that can result in neurological and neurodevelopmental diseases, and cancer (Poduriet al., 2013).

1.6 Centromere Associated Protein E

Centromere Associated Protein E (CENP-E) is a plus-end kinesin motor protein in mammalian cells that is responsible for chromosomal movement and spindle elongation. This protein functions in chromosome congression to the equator of the cell (Sardar et al., 2010). It consists of three major domains: a dimeric coiled coil intervening region, an amino-terminal motor domain, and a carboxy-terminal MT binding domain (Grancell and Sorger, 1998). The motor domain of CENP-E allows it to travel down MTs towards the KTs post-NEBD (Yao et al., 2000). The plus-end motor activity is fueled by ATP hydrolysis in prometaphase and only binds MTs at the surface of kinetochores in anaphase. CENP-E is located at the outer kinetochore extending about 100nm from its surface and remains there throughout the rest of the phases in mitosis. It binds to MTs at the surface of KTs with its MT-binding domain (Musinipally et al., 2013). Unlike typical plus end-directed kinesins, CENP-E also transitions in a minus-direction. The minus-directed transition of mono-oriented chromosomes towards the metaphase plate is achieved by spindle depolymerization that is fueled by GTP hydrolysis (Grancell and Sorger, 1998). However, depletion of CENP-E does not hinder chromosomes from transitioning to the spindle equator. Even though chromosomal transition is not arrested, the loosely bound MTs to their KTs do increase the chances of chromosome mis-segregation (Putkey et al., 2002) and aneuploidy in daughter cells (Kim et al., 2008). This suggests that CENP-E functions in KT-MT binding.

During metaphase CENP-E functions at the level of the SAC. Its conformational changes at the surface of the KT can cause SAC amplification by interacting via its motor domain with BubR1. This interaction enhances the autophosphorylation activity of BubR1 which is important for the attachment of MT to KT (Foltz et al., 2006). The enhancement of BubR1 kinase activity by CENP-E is not critical to the progression of mitosis since CENP-E depletion does not result in the inhibition of APC (Zhao et al., 2011). The activity of BubR1 decreases to basal levels without causing mitotic arrest at anaphase entry (Weaver et al. 2003). Mitotic arrest can occur depending on the number of

unattached KTs present. If one KT is unattached in HeLa cells, mitotic arrest does not occur. Once 7 unattached KTs are present in HeLa cells, mitotic arrest occurs as CENP-E can form a ternary complex with BubR1 and can silence its kinase activity (Mao et al., 2005). This interaction activates the mitotic checkpoint complex, resulting in the inhibition of APC (Guo et al., 2012). Xenopus extracts have resulted in no mitotic arrest through this mechanism (Weaver et al. 2003) making this process cell-type dependent.

TABLE 1.1:

Mammalian and yeast TRAPP subunit nomenclature

S. cerevisiae TRAPP subunit (KDa)	Mammalian TRAPP subunit (KDa)
Bet5p (18)	TRAPPC1 (17)
Tca17p (17)	TRAPPC2L (16)
Trs20p (22)	TRAPPC2 (16)
Bet3p (22)	TRAPPC3, TRAPPC3L (20)
Trs23p (23)	TRAPPC4 (24)
Trs31p (31)	TRAPPC5 (21)
Trs33p (33)	TRAPPC6a,b (19,15)
Trs65p (65)	
Trs85p (85)	TRAPPC8 (161)
Trs120p (120)	TRAPPC9 (140)
Trs130p (130)	TRAPPC10 (142)
	TRAPPC11 (129)
	TRAMM (79)
	TRAPPC13 (40)

Proteins on the same row indicate homologues; empty cells indicate no homologues detected in databases.

Project: Cdk1 has a role in phosphorylating TRAMM

TRAMM was originally identified as a protein that co-precipitates with the TRAPP (transport protein particle) complex that functions in membrane trafficking. Recent work in our laboratory suggested a role for this protein in mitosis, specifically in chromosome congression prior to metaphase (Figure 1.1(A), Figure 1.1(C)). In early stages of mitosis, TRAMM is post-translationally modified by phosphorylation (Figure 1.1(B)). Knockdown of the protein causes it to affect the localization of various kinetochore proteins with the strongest effect on CENP-E. The two proteins were shown to interact in vitro using a yeast two hybrid assay (Milev et al., 2015).

In this study, I will use a co-immunoprecipitation assay to check whether the in vitro interaction between TRAMM and CENP-E also occurs in vivo. Using various inhibitors of mitotic kinases, I will identify the kinase responsible for the phosphorylation of TRAMM. Furthermore, I will also use bioinformatics tools to predict and analyze the structure of TRAMM. Finally I will express and purify the recombinant form of TRAMM in a homogeneous monodispersed protein sample as an initial step towards future structural analysis via crystallization. This study will allow us to better understand the unique role of TRAMM in mitosis.

Chapter 2: Materials and Methods

2.1 Buffers and solutions

All buffers and solutions used in this project are listed in Table 2.1 at the end of the Materials and Methods section.

2.2 Protein analysis techniques

2.2.1 Protein expression and purification:

E. coli Arctic Express ® cells were transformed with a recombinant form of TRAMM that was inserted into pDEST-17 plasmid (containing a 6x His tag). The cells were grown at 37°C overnight on Luria Bertani (LB) agar plates supplemented with ampicillin (amp) (100 mg/mL). A single colony was used to inoculate a 20 mL starter culture of LB+amp media that was incubated with shaking at 37°C overnight. 500 mL of LB+amp media was inoculated with the starter culture (with or without 10 mM $MgCl_2$), then incubated at 30°C with shaking until the OD at 600 nm reached 0.7-0.8. Expression of recombinant TRAMM was then induced by addition of IPTG (Isopropyl β-D-1-thiogalactopyranoside) to a final concentration of 1 mM. After 24 hours shaking at 12°C, cells were harvested by centrifugation at 10,000 × g for 10 min at 4°C. Pellets containing recombinant TRAMM were re-suspended in 35 mL of lysis buffer containing 7µl of 0.5 M AEBSF (protease inhibitor). This was followed by programmed sonication (10 sec on/10 sec off for 2 minutes). Lysates (with or without 5 units of DNAse I from Thermo Scientific Lot 00152435) were cleared at 30,000 × g for 30 min at 4°C. During this time the Ni^{2+}-beads were prepared as follows. A 50% slurry of nickel beads was resuspended in lysis buffer. The mixture was centrifuged at 270 × g for 2 minutes at 4°C. The buffer was aspirated leaving a small volume above the beads. After 3 washes, the beads were resuspended in lysis buffer and added to the supernatant obtained as described above. Note that 500 µL of washed nickel beads, which is equivalent to 1 mL of 50% slurry solution were incubated with each sample for 1 h. The mixture was passed through a gravity column to collect the beads and the column was washed once with 10 mL of lysis buffer and twice with 15 mL of washing

buffer. TRAMM was eluted by incubation for 5 minutes with 0.5 mL elution buffer before being collected.

2.2.2 Co-immunoprecipitation (IP):

For each sample, 1 mg of HeLa cell lysate (collected from a 10 cm dish) was mixed with 2 µg of anti-GFP IgG and incubated for 2 h on ice. During this time Protein-G agarose beads were prepared as follows. A 50% slurry solution of protein-G agarose beads was resuspended in lysis buffer then centrifuged for 30 seconds at 5000 rpm at 4°C. The supernatant was removed without disturbing the pellet that contains the beads. The washing process was repeated three times before the beads were re-suspended in PBS and added to the samples (10 µl of beads per sample, which is equivalent to 20 µl of 50% slurry solution). The mixture was left shaking for 1 hour at 4°C. The beads in the mixture were washed with lysis buffer 3 times. After the last wash was completed and the buffer was aspirated, 20 µL of 1x sample buffer containing 5% BME (B-mercaptoethanol) was added and the sample was incubated at 96°C for 2 minutes. Before freezing at -20ºC, the beads in the sample were pelleted at 13000 rpm for 2 minutes.

2.2.3 Mass spectrometry:

After His-tagged TRAMM was purified and subjected to SDS PAGE, the Coomassie blue stained gel was rinsed with MilliQ H_2O. The desired band was excised with a clean scalpel and diced into small pieces. Coomassie destaining was performed by the addition of 100 µL of NH_4HCO_3 in 50% methanol. The mixture was centrifuged briefly and the supernatant was discarded. 100 µL of 100% acetonitrile (ACN) was added to the gel particles and the mixture was incubated for 5 minutes with occasional mixing. The mixture was centrifuged and the supernatant was discarded. Gel particles were covered with 100 µL of 10 mM DTT and the mixture was incubated at 50°C for 30 minutes. Brief centrifugation was performed and the liquid was discarded. The particles were alkylated by the addition of 100 µL of 55 mM iodoacetamide. After 30 minutes of incubation at room temperature, the mixture was centrifuged and the liquid was removed. The particles were dehydrated using 100 µL ACN and dried in a speed vac for 20 minutes. After drying, the particles were incubated on ice with 10 µL of 20

ng/µL trypsin for 10 minutes with occasional vortex mixing. Excess trypsin was removed and 30 µL of 50mM NH_4CO_3 was added. The mixture was incubated for 18 hours at 37°C to allow for protein digestion. 50 µL of H_20 was added to each sample and the mixture was vortexed for 2 minutes, and then centrifuged at 5000 rpm for 30 seconds. The supernatant containing tryptic peptides was transferred to a newly labeled tube. The volume was reduced to 15 µL using a speed vac. Samples were cleaned using a C18 ziptip (Millipore) and subjected to HPLC-MS. For HPLC a Spursil Column C18, 3mm particle size, 150mm long, 2.1mm diameter from Agilent model 1200 was used. For mass spectrometric analysis the sample was injected into a Waters QTOF3 (also known as an Ultima) at a mass range of 400Da to 2000Da with a dissolving temperature of 300°C at a flow rate of 10µL/min.

2.2.4 Dynamic Light Scattering:

Purified recombinant His-tagged TRAMM protein was subjected to size exclusion chromatography (described in 2.2.8) and 0.5mL fractions were collected. The fractions that represented the TRAMM peak (fractions 20-25) were combined to reach a volume of 2.5mL. The mixture was concentrated by using an Amicon ultra-4 centrifugal filter unit that was centrifuged at 4000 × g for 5 minutes at 25°C to obtain a final volume of 50 µL. The mixture was then filtered with a 0.45-micron filter syringe. The filtered solution was subjected to dynamic light scattering using a DynaPro Nanostar instrument at 25°C and laser power of 100 crescents.

2.2.5 Bradford Assay:

Using Ultrospec 2100pro spectrophotometer at 595 nm, a standard calibration curve was prepared from known quantities of BSA. Five different points were used in each standard curve corresponding to 1,2,4,6 and 10 µg of BSA. 10 µL of the protein sample was diluted with 1 mL of Bradford reagent. The protein sample concentration was determined by comparison with the standard curve at an OD of 595 nm.

2.2.6 Western blotting:

Samples were subjected to electrophoresis on 8%, 10%, 12% or 15% Polyacrylamide

gels at 120V. Proteins were transferred to nitrocellulose membranes for 1 h at 100 V in cold transfer buffer. The membranes were blocked with 5% skim milk for 1 hour and then incubated with primary antibody in PBSt (concentrations mentioned in the antibody section below) for 2 hours. After 3 washes with PBSt for 5 minutes each, the membranes were incubated with the secondary antibody (anti-mouse or anti-rabbit conjugated to horseradish peroxidase) at a dilution of 1:10000 for 1 hour. Finally, ECL reagent (Amersham Life Science) was added in the dark room and incubated with the membrane for 2 minutes and then exposed to photographic film at different time exposures (1 sec–15 min) to produce the desired exposure.

2.2.7 Size exclusion chromatography:

Recombinant His-tagged TRAMM protein was purified as described above and 100 µg of the 150 mM imidazole elution was loaded onto a Superpose 6 column and fractionated in gel filtration buffer at a rate of 0.5 mL/min. Fractions of 0.5 mL were collected and resolved by SDS-PAGE and Coomassie blue staining.

2.3 Tissue culture techniques

2.3.1 Cell culture:

HeLa or HEK293T cells were grown in Dulbecco's Modified Eagle Medium (DMEM) supplemented with 10% fetal bovine serum (FBS) at 37°C in a humidified incubator with 5% CO_2. Cells were either asynchronously growing or synchronized at different stages of the cell cycle as described below.

2.3.1.1 Double thymidine treated cells:

HeLa cells plated at 25-30% confluency (300,000-350,000 cells per 10 cm dish) were treated with 2 mM thymidine for 18 hours, washed 2 times with PBS, and then released into medium for 6 hours. HeLa cells were subjected to another treatment of 2mM thymidine for 16 hours before they were either harvested or released into DMEM.

2.3.1.2 Nocodazole treated cells:

After 3 hours of the second thymidine release (as mentioned above), 100 ng/mL of Nocodazole was added into the medium. After 9 hours of the nocodozole treatment, cells were treated with one of the following kinase inhibitors: 100 nM BI-2536 (a Plk1 inhibitor), 2 µM ZM-44743 (an Aurora A, B, C inhibitor), 9 µM R0-3306 (a Cdk1, 2 inhibitor), or left untreated before cells were harvested at different time points as mentioned in the results (section 3.2).

2.3.1.3 Colcemid treated cells:

When HeLa cells (plated on a 10 cm dish) reached 80% confluency, they were treated with 5 µg/mL of colcemid for 17 hours before they were washed 3 times with PBS before harvesting.

2.3.2 HeLa cells harvesting:

Mitotic cells treated with colcemid or nocodazole were directly collected in the medium since they were easily removed from the plastic dishes. Non-mitotic cells were trypsinized for 2 minutes after which the cells were washed with PBS. Both mitotic and non-mitotic cells were pelleted at 1900 rpm for 2.5 minutes at 4°C, and washed with PBS before they were pelleted again and finally lysed with lysis buffer. Cells were stored at -20°C until they were subjected to western blots.

2.3.3 Lambda phosphatase treatment:

HeLa total cell lysates were centrifuged at 16000 rpm for 20 minutes at 4°C to remove the cell debris. Cell extracts were incubated for 2 hours at 30°C with Lambda phosphatase solution (containing 400 units of Lambda phosphatase, 1x NEBuffer for protein metallophosphatases and 1mM $MnCl_2$) from Bio England Biolabs (P0753S). The reaction was terminated by the addition of 4x SDS sample buffer followed by boiling for 2 minutes at 96°C.

Table 2.1 List of buffers and solutions used in this study

Reagent name	Components
Nickel-bead purification lysis buffer	50mM Tris-base pH 8.5, 5% v/v glycerol, 1% Triton X-100, 0.3M NaCl, 10mM BetaMercaptoethanol
Nickel-bead purification wash buffer	50mM Tris-base pH 8.5, 200 mM NaCl, 5mM imidazole
Nickel-bead purification elution buffer	50mM Tris-base pH 8.5, 1mM BME, 200 mM NaCl, 50-200 mM imidazole
PBS	0.061% w/v Na_2HPO_4, 0.8% w/v NaCl, 0.02% w/v KCl, 0.02% w/v KH_2PO_4 pH 7.3
PBSt	PBS with 0.1% v/v Tween-20
4x sample buffer	80 mM Tris-HCl pH 6.8, 0.1% bromophenol blue, 5% v/v Betamercaptoethanol, 10% v/v glycerol, 2% w/v SDS
SDS-PAGE running buffer	25mM Tris-base, 200mM glycine, 0.1% SDS
Western blotting transfer buffer	Tris-base, 200mM glycine, 25mM, 20% methanol
Mammalian cells lysis buffer	50mM Tris-base pH 7.2, 1% Triton X- 100(v/v), 0.5mM EDTA, 1mM DTT, 150mM NaCl, 2 tablets of Phospho-Stop (Roche) per 10mL, 1 tablet of protease inhibitor cocktail (Roche).
Gel filtration buffer	50mM Tris-base pH 7.2, 0.5mM EDTA, 150mM NaCl
Luria Bertani (LB)	0.5% w/v yeast extracts, 1% w/v tryptone, 1% w/v NaCl

Table 2.2 List of antibodies used in this study

Antigen	Type	Host	WB dilution	Size	Catalog number	Source
Cyclin B1	P	r	1:1,000	58	4138	Cell Signaling
Phospho-histone H3	M	m	1:1,000	17	3377	Cell Signaling
TRAMM	P	m	1:1,000	78	Ab27076	Abcam
TRAMM	P	r	1:1,000	78	N/A	Sacher laboratory
Tubulin	M	m	1:5,000	50	Ab27076	Abcam
GFP	M	m	1:1,000	27	Ab1218	Abcam

Protein sizes are indicated in kilodaltons. M, monoclonal; P, polyclonal; N/A, not applicable; r, rabbit; m, mouse; WB, western blotting.

Chapter 3: Results

3.1 TRAMM associates directly or indirectly with CENP-E in vivo

TRAMM plays a role in mitosis and its depletion results in a chromosome congression failure. This is caused by the mislocalization of some kinetochore proteins and the strongest effect was seen for CENP-E. Results of this yeast two-hybrid assay suggested a direct interaction between TRAMM and CENP-E (Milev et al., 2015).

To confirm that the interaction that was seen by yeast two-hybrid also occurs in vivo, lysates prepared from human embryonic kidney (HEK293T) cells stably expressing GFP-tagged CENP-E were used for Co-IPs. HeLa cells were used as negative controls. Reasoning that the expression of CENP-E increases during mitosis (as compared to interphase cells) (Testa et al., 1994), lysates from asynchronous cells or colcemid treated (mitotic) cells were incubated with anti-GFP to precipitate CENP-E and then probed for TRAMM. As compared to the control HeLa cells, a greater amount of TRAMM co-precipitated with CENP-E indicating that it associates with CENP-E directly or indirectly in vivo (Figure 3.1). More interestingly, this association increased in mitotic cells when compared to interphase cells. This result is consistent with the yeast two-hybrid result showing that TRAMM does not only interact with CENP-E in vitro, but the two also associate directly or indirectly in vivo.

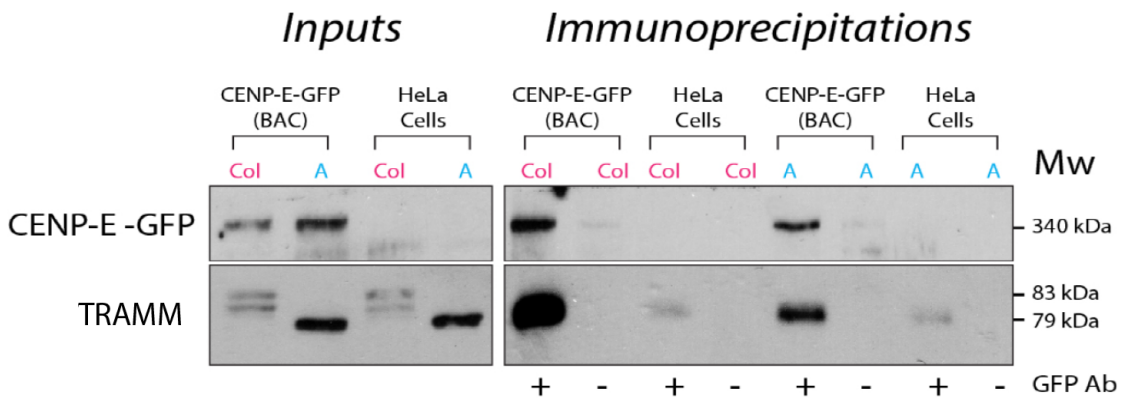

Figure 3.1 TRAMM associates directly or indirectly with CENP-E invivo.

Bacterial artificial chromosome (BAC) cell line expressing CENP-E-GFP in HEK293T and HeLa cells (negative control) were co-immunoprecipitated using GFP antibody. The left panel represents 10% of the inputs and right panels represents the IPs. Cells were either left asynchronous (A) or treated with colcemid (Col) to arrest cells in mitosis. Samples were probed for GFP and TRAMM.

3.2 Phosphorylation of TRAMM is Cdk1 dependent

TRAMM is phosphorylated early in mitosis and dephosphorylated at the onset of anaphase. This phosphorylation leads to the appearance of a slower migrating doublet at ~83 KDa as compared to a faster-migrating band at ~79 KDa of non-phosphorylated TRAMM (Milev et al., 2015). In order to determine the kinase responsible for phosphorylating TRAMM during mitosis, we focused on the three main mitotic kinase families: Cdks, Aurora kinases, and Plks.

HeLa cells were arrested at the G1/S boundary by thymidine treatment and then released into medium containing nocodazole (to arrest the cells at prometaphase). HeLa cells were then treated with BI-2536 (a Plk1 inhibitor) in Figure 3.2(A), ZM-44743 (an Aurora A, B, C inhibitor) in Figure 3.2(B), R0-3306 (a Cdk1, 2 inhibitor) in Figure 3.2(C), or left untreated in Figure 3.2(D). Figure 3.2 shows the results of HeLa cells that were collected at various times following double thymidine release, lysed and subjected to western blots. Samples were probed for TRAMM, phospho-Histone 3 (mitotic marker), and Tubulin (loading control). HeLa cells that were collected 3h following the release from double thymidine treatment showed no signs of phosphorylation because the cells were still in interphase (phospho-H3 is absent). At 11h following release, HeLa cells showed a slower migrating form representing the phosphorylation of TRAMM during mitosis (phospho-H3 is present). When the cells were only treated with nocodazole (control condition), the phosphorylation of TRAMM was present from 11h to 13h (Figure 3.2(D)). Similar results were seen in Figure 3.2(A) and Figure 3.2(B) upon the treatment with BI-2536 and ZM-447439, respectively. In contrast, when HeLa cells were treated with RO-3306 TRAMM was phosphorylated at 11h but not at subsequent time points (Figure 3.2(C)). The dephosphorylation that occurred in the presence of the Cdk inhibitor but not in the presence of the Plk or Aurora kinase inhibitors suggests that phosphorylation of TRAMM at mitosis is Cdk-dependent. At a concentration of 9 μM, RO-3306 inhibits Cdk1 and Cdk2. Cdk2 is mainly involved in interphase while Cdk1 is one of the main protein kinases orchestrating mitosis. This strongly suggests that phosphorylation of TRAMM is Cdk1-dependent.

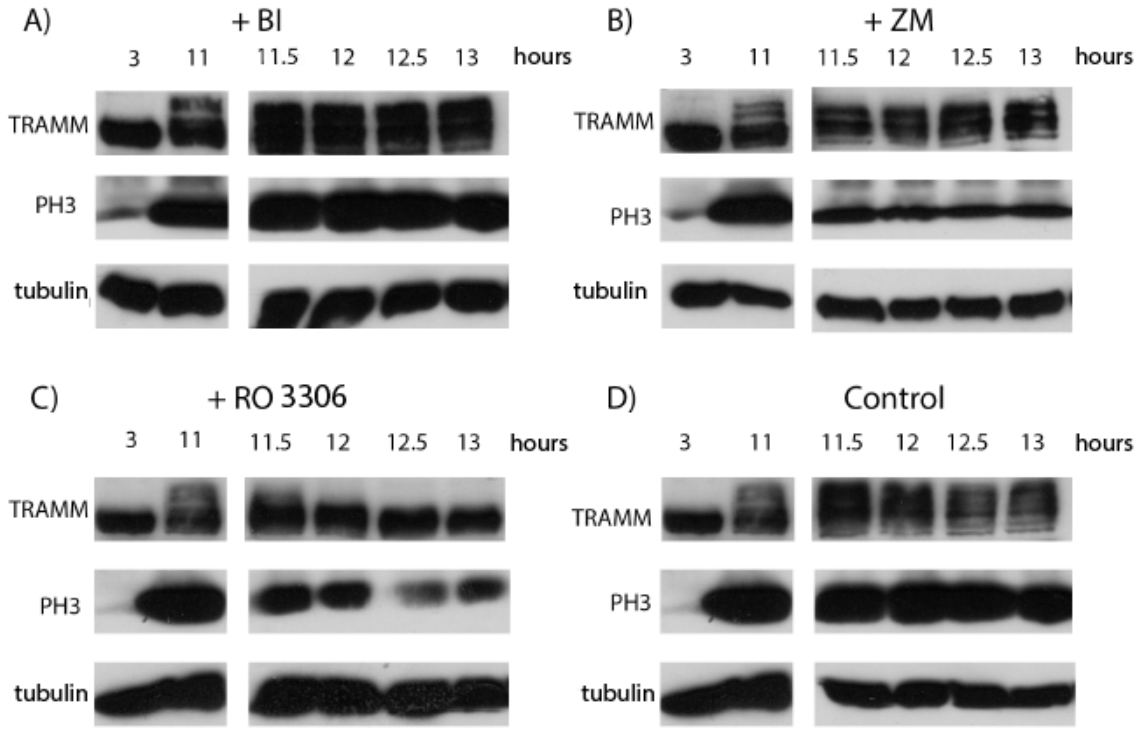

Figure 3.2 Phosphorylation of TRAMM is Cdk1 dependent. Western blot analysis of HeLa cells collected at different time indicated in hours after double thymidine treatment. Note that all blots were subjected to the same exposure time. As indicated in materials and methods section cells were treated with various mitotic protein kinase inhibitors after 11h of the second thymidine release: A) BI-2536 (Plk1 inhibitor); B) ZM0447439 (Aurora A,B,C inhibitor); C) RO3306 (Cdk1,2 inhibitor); D) no inhibitor was added. Antibodies used in western blots are: Anti TRAMM; Anti PH3 (phospho-histone 3); Anti tubulin.

3.3 Prediction of the structure of TRAMM and possible phosphorylation sites

Solving the structure of TRAMM is an important step to determining its function (Freeman et al., 2002). However, in the absence of the structure, bioinformatics tools can give us some limited information on TRAMM. According to UniProt database TRAMM contains 4 distinct TPR repeats in the carboxy half of the protein (Figure 3.3 (A)) and 12 overlapping TPR domains according to KEGG database (Figure 3.3(B) and Figure 3.3(C)). The Tetratricopeptide repeat (TPR) domain is a structural motif that consists of degenerate 34 amino acid repeats. These alpha helix pair repeats fold together forming scaffolds to mediate protein-protein interactions (Blatch et al., 1999). Interestingly, other cell division proteins such as APC subunits including cdc16 and cdc23 contain TPR motifs for their unique functions in facilitating protein-protein interactions, and the assembly of multiprotein complexes (Passmore et al., 2005). Phyre 2 database was also utilized for performing the structural analysis of TRAMM. According to Phyre 2, the secondary structure showed 53% unstructured regions, 44% structured helices and 1% β strands. Moreover, tertiary structural analysis (Figure 3.4(A)) revealed that the TPR domains are exposed and not shielded by the amino terminus, thus facilitating protein-protein interactions. As mentioned above, TRAMM is predicted to be largely unstructured and studies have shown that unstructured regions are often involved in posttranslational modifications, such as phosphorylation (Dyson et al., 2005).

I next sought to determine which sites of TRAMM are potenitally phosphorylated during mitosis. Uniprot database revealed 2 possible phosphorylation sites: 109 and 184 (Figure 3.3(A)). To precisely predict the possible sites of phosphorylation, several phosphoproteomic studies (Milev et al., 2015; Dephoure et al., 2008; Kettenbach et al., 2011; Mayya et al., 2009) were mined for TRAMM phosophorylation (Figure 3.4(B)). This revealed 5 sites of phosphorylation that occur in vivo. Consistent with results from Figure 3.4(A), Figure 3.4(B) predicts amino acids 109 and 184 as possible sites of phosphorylation and adds 3 extra possible phosphorylation sites: 107, 127 and 182. All 5 sites of phosphorylation: 107, 109, 127, 182 and 184 are located in the unstructured N-terminal portion of the protein. Now that I have determined the 5 possible sites of phosphorylation, I checked whether any of these sites contain Cdk1 consensus motif (S/T P) (Dephoure et al., 2008). Interestingly residues 107, 109 and 182, conform

to the Cdk1 consensus motif (S/T P). This is consistent with the results shown in Figure 3.2.

Figure 3.3 (A)

Motif id	From	To	Definition	E value
pf:TPR_2	547	577	Tetratricopeptide repeat	0.12
pf:TPR_12	547	609	Tetratricopeptide repeat	0.026
pf:TPR_1	547	577	Tetratricopeptide repeat	0.0019
pf:TPR_6	547	577	Tetratricopeptide repeat	0.0023
pf:TPR_16	552	605	Tetratricopeptide repeat	0.14
pf:Cohesin_load	573	731	Cohesin loading factor	0.1
pf:TPR_12	582	651	Tetratricopeptide repeat	0.00037
pf:HrpB1_HrpK	602	667	Bacterial type III secretion protein (HrpB1_HrpK)	0.051
pf:Coatomer_E	617	691	Coatomer epsilon subunit	0.00067
pf:TPR_2	623	653	Tetratricopeptide repeat	0.0075
pf:TPR_9	629	686	Tetratricopeptide repeat	0.15
pf:TPR_16	630	685	Tetratricopeptide repeat	0.0017
pf:TPR_19	631	690	Tetratricopeptide repeat	5.8e-06
pf:TPR_17	643	672	Tetratricopeptide repeat	0.13
pf:TPR_2	656	687	Tetratricopeptide repeat	0.32

Table 3.1

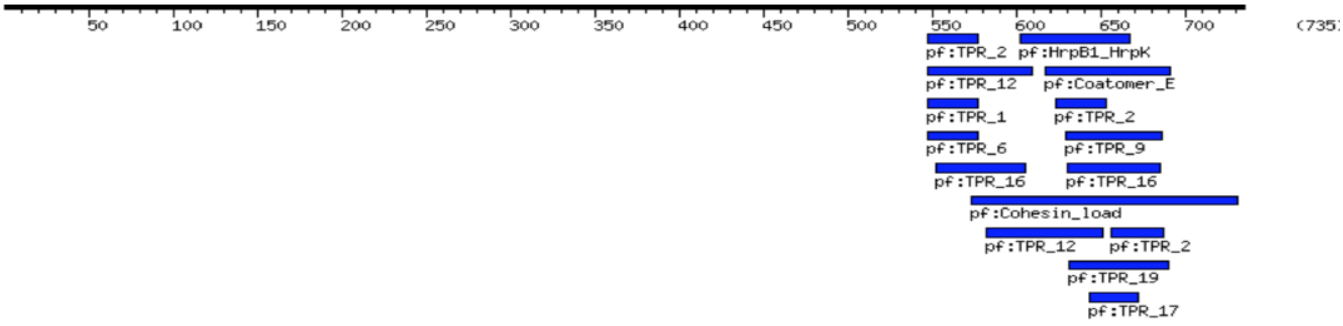

Figure 3.3 (B)

Figure 3.3 (A) Schematic representation of TRAMM's conserved motifs extracted from Uniprot database. Table 3.1 and Figure 3.3 (B) Conserved motifs extracted from KEGG analysis.

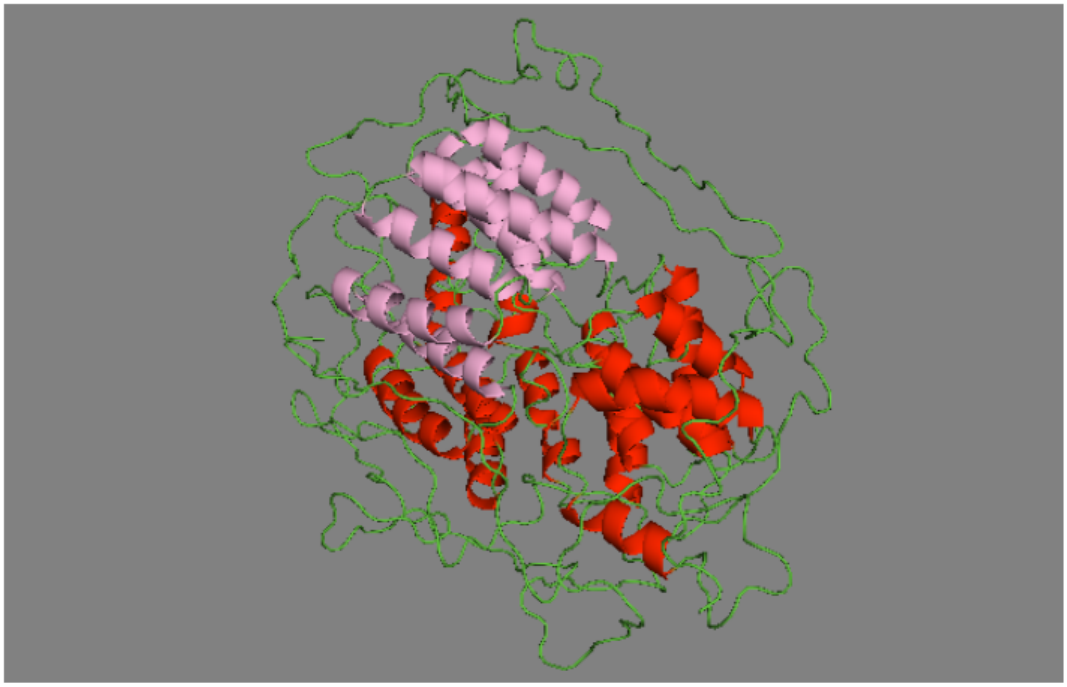

A

Phosphorylation sites identified in TRAMM

Residue	Peptide	Source
T107	PEPAGTPSPSGEAD	Milev et al., 2015; Dephoure et al., 2008
S109	PEPAGTPSPSGEAD	Milev et al., 2015; Dephoure et al., 2008
S127	DAAPSSGGAPR	Milev et al., 2015; Dephoure et al., 2008
S182	PQMVKSPSFGGAS	Milev et al., 2015; Mayya et al., 2009; Kettenbach et al., 2011
S184	PQMVKSPSFGGAS	Milev et al., 2015; Dephoure et al., 2008; Mayya et al., 2009

B

Figure 3.4 Prediction of TRAMM tertiary structure and possible phosphorylation sites. (A) Tertiary structure prediction from Phyre 2 showing unstructured region in green, helices in red and TPR repeats in pink. (B) Possible phosphorylation sites of TRAMM extracted from different studies.

3.4 Optimization of TRAMM recombinant protein purification

One way to address the function of TRAMM is to determine its three-dimensional structure by techniques such as small-angle x-ray scattering, nuclear magnetic resonance or X-ray crystallography. The first step towards elucidating the three-dimensional structure is purifying the protein of interest. Such a protein could also be used for generating anti-TRAMM antibody. Moreover, the purified protein could be used in an in vitro kinase assay to confirm that Cdk1 has a role in phosphorylating TRAMM (section 3.2). Recombinant TRAMM was expressed in BL21 (DE3) cells but the protein was found to be in the insoluble fraction. Reasoning that proteins tend to fold better at lower temperatures, I next tried to express the protein in Arctic Express (DE3)® cells. These cells were used since they contain two low-temperature chaperones (Cpn10 and Cpn60) to aid in protein folding. The expression and purification of TRAMM in Arctic Express cells, resulted in the presence of two bands as shown in Figure 3.5(A): a slower migrating polypeptide that was at the molecular size of TRAMM (79 KDa) and a faster migrating species. The two bands were excised, trypsinized and subjected to mass spectrometry. Mass spectrometry results of the slower migrating polypeptide are shown in Figure 3.6(A). Peaks were collected and graphs representing M/Z versus intensity (data not shown) were utilized to conclude the mass of fragmented peptides. Utilizing the masses of the fragmented peptides, and with the help of database searches, this polypeptide was identified as our protein of interest, TRAMM. Mass spectrometry also revealed that the faster migrating species was an undesired bacterial-expressed contaminant belonging to the ArnA gene (data not shown). The issue of contamination was addressed by the treatment with divalent cations ($MgCl_2$) (based on personal communication with Eduardo A. Ceccarelli on ResearchGate) that had the ability to suppress the expression of ArnA in E. coli. This resulted in the purification of just the TRAMM protein (Figure 3.5(B)). However, this treatment led to the appearance of a smear on the top of our band of interest. Due to its high molecular weight and smeary appearance, it was suspected to be DNA. Therefore, lysates were treated with DNAseI. The combination of $MgCl_2$ and DNAseI treatments resulted in a clear single band (Figure 3.5(C)).

A western blot utilizing a commercially-available TRAMM antibody was conducted on the

protein sample to confirm the mass spectrometry results. Figure 3.6(B) shows that anti-TRAMM was specifically binding to the protein sample, which resulted in a 79 kDa band corresponding to the molecular size of TRAMM). This band was absent in the negative control (bovine serum albumin). All together mass spectrometry, as an unbiased technique, and western blotting conclude that the purified protein sample is TRAMM.

The purified protein was used for generating an anti-TRAMM antibody, which was utilized for probing all subsequent western blots. The homemade antibody recognizes the same polypeptide as the commercial anti-TRAMM antibody, where it is able to detect TRAMM in its phosphorylated state (HeLa cells treated with colcemid but not lambda phosphatase) and non-phosphorylated form (Lambda phosphatase treated HeLa cells) (Figure 3.6(C)).

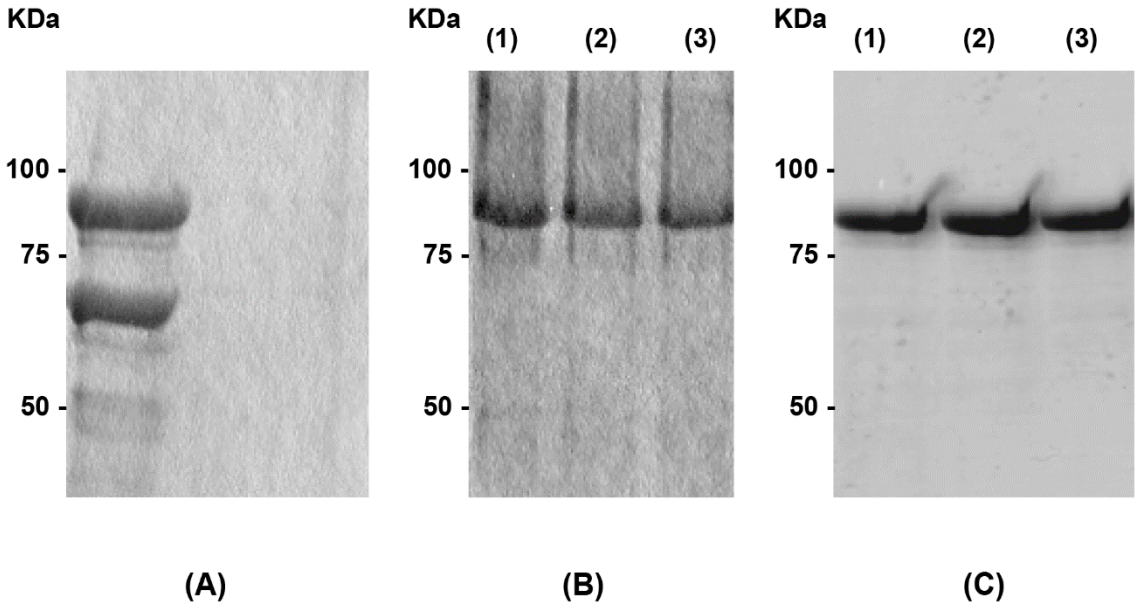

Figure 3.5 SDS-PAGE followed by Comassie bleu staining of purified TRAMM. (A) Purification process was done in the absence of $MgCl_2$, showing TRAMM (the higher band) and another undesired polypeptide. (B) Purification process was done the presence of $MgCl_2$, but without DNAse treatment showing a smear on the top of the band. Lanes (1), (2) and (3) represent different elutions with 150mM imidazole elution buffer. (C) Purification process was in presence of $MgCl_2$ and DNAse. Lanes (1), (2) and (3) represent different elutions with 150mM imidazole elution buffer.

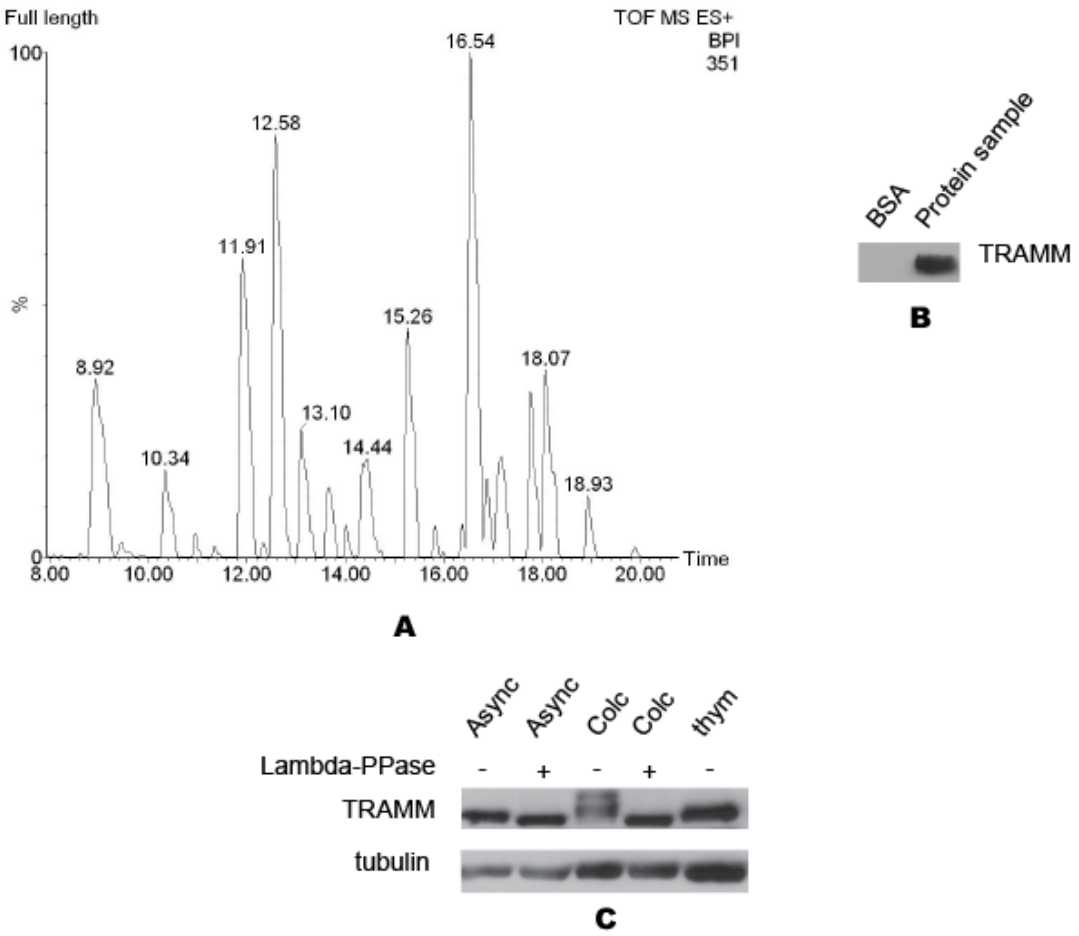

Figure 3.6 Confirmation of TRAMM and antibody production. (A) Mass spectrometry data showing data showing the variation of time as function of the intensity of fragmented peptides. (B) Western blot probed with anti-TRAMM for protein sample and negative control BSA (Bovine serum albumin). (C) Western blot of asynchronous, colcemid treated and thymidine arrested HeLa cells. HeLa cells were either treated with Lambda phosphatase (+), or left untreated. Blots were probed for TRAMM using homemade antibody.

3.5 Recombinant purified TRAMM protein analysis by dynamic light scattering

The polydispersity of a protein sample represents the protein's particle size distribution width. A protein sample with less than 20% polydispersity is considered to be monodispersed (Price et al., 2009). Figure 3.7(A) represents the initial observation of the dynamic light scattering (DLS) of a TRAMM protein sample, showing 2 peaks at $3x10^6$ counts/sec with radius R=39.5nm and R=107.6nm, respectively. This result does not represent a protein of molecular weight= 79KDa. The R is too large and the counts are too high. To address this problem the buffer containing TRAMM was changed by fractionating the sample on a size exclusion (Superpose 6) column removing B-mercaptoethanol and imidazole. Fractions collected from the size exclusion column were subjected to SDS-PAGE and Coomassie blue staining (Figure 3.7(B), top panel) revealing a band at the desired molecular size of TRAMM, mainly in fractions 20-25. These fractions were combined and concentrated, and then analyzed by DLS. The resulting sample was at 27.4% polydispersity, which is still considered to be a polydispersed sample >20% polydispersity, as shown in Figure 3.7(C). Reasoning that the elution by size exclusion chromatography was occurring at a size greater than that expected for a 79kDa polypeptide, we suspected the presence of high molecular weight particles in the solution besides TRAMM. For the purpose of removing the undesired high molecular weight particles from the solution; the sample from Figure 3.7(C) was filtered using a 0.45 micron filter to yield the solution analyzed in Figure 3.7(D). Results in Figure 3.7(D) yielded 16.5% polydispersed species at R=15.4nm that is reasonable for a 79KDa protein. The monodispersed protein (<20% polydispersity) obtained from Figure 3.7(D) was subjected to western blotting and probed with the homemade anti-TRAMM antibody. While the negative control (purified TRAPPC2) did not show any band at 79 KDa, the purified sample showed a clear band of the expected size (Figure 3.7(B), bottom panel), confirming that the monodispersed protein analyzed in Figure 3.7(D) is TRAMM. As a result, Figure 3.7 shows successful optimization and transition of the polydispersed protein sample of purified TRAMM to a monodispersed protein sample. A monodispersed protein sample is a strong indicator of successful crystallization of the protein, which could reveal its three-dimensional structure (Goh et al., 2004).

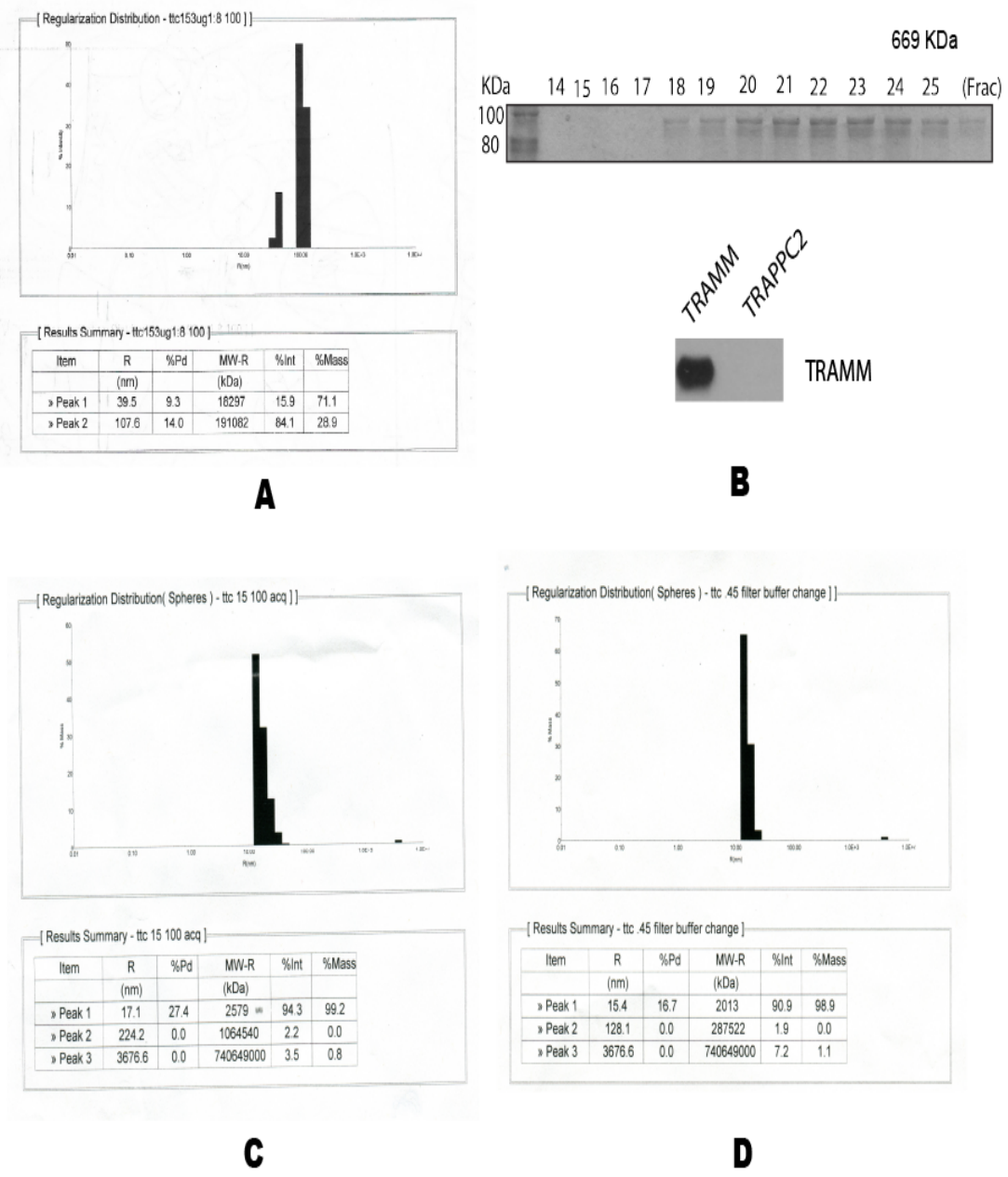

Figure 3.7 Recombinant purified TRAMM protein analysis by dynamic light scattering. (A) Graph representing DSL results of purified TRAMM protein sample in its initial elution buffer. (B) Top: Size exclusion chromatography of purified recombinant TRAMM. Eluted protein at 150mM imidazole was fractionated on Superpose 6 size exclusion column and subjected to Coomasie blue staining. Molecular size standard is

indicated on top; bottom panel: Western blot probed with anti-TRAMM for TRAMM protein sample (after changing the buffer and filtering the sample using 0.45 micron filter as described in materials and methods section 2.2.5) and negative control TRAPPC2. (C) Graph representing DSL results of purified TRAMM protein sample in elution buffer without DTT and imidazole. (D) Graph representing DLS results of purified TRAMM protein sample in new buffer and filtered using 0.45 micron filter.

Chapter 4: Discussion

The TRAPP complex was initially discovered as a tethering factor involved in membrane trafficking (Sacher et al., 1998). Recent work in our laboratory suggests that TRAMM is involved in mitosis (Milev et al., 2015). Size exclusion chromatography of HeLa cells revealed that TRAMM, which belongs to the TRAPP complex during interphase, dissociates from the complex and shifts to lower molecular size fractions during mitosis. The mechanism by which TRAMM dissociates from the TRAPP complex during mitosis is still unclear. In mitosis, TRAMM is post-translationally modified by phosphorylation (Milev et al., 2015). Phosphorylation can cause conformational changes that could affect protein-protein interactions and thus allow proteins to be dissociated from their complexes (Nishi et al., 2011). This would provide a mechanism for TRAMM to perform its role during mitosis and to dissociate from the TRAPP complex. Alternatively, TRAMM could dissociate from the complex by a different mechanism, which is independent of the phosphorylation. Interestingly, TRAMM-5D (a phosphomimetic mutant that contained all five potential phosphorylation sites changed to aspartic acid residues) was able to recruit more CENP-E to the kinetochores than TRAMM-5A (a mutant that had all five phosphorylation sites changes to nonphosphorylatable alanine residues). As compared to TRAMM-5A, TRAMM-5D showed a reduced ability to suppress the increase in mitotic index induced by TRAMM depletion. These results could suggest that although the phosphorylation of TRAMM is not necessary, it needs to be reversible for proper function. In this study, I show that Cdk1 is most likely the kinase responsible for the phosphorylation of TRAMM. The dephosphorylation observed when Cdk1 was inhibited could be explained by the fact that in mitosis there is a balance between kinases and phosphatases. It is this balance that orchestrates the cell cycle and allows the cell to progress throughout mitosis (Barr et al., 2011). Upon altering the kinase-phosphatase equilibrium by inhibiting Cdk1, which is the kinase responsible for phosphorylating TRAMM, the corresponding phosphatase would be capable of dephosphorylating TRAMM.

Several facts could support that TRAMM is phosphorylated by Cdk1. Cdk1 is a major mitotic kinase that phosphorylates more than 200 cell cycle related proteins mainly involved in triggering mitotic entry and progression with maximal activity at metaphase

(Errico et al., 2010; Ubersax et al.,2003). In parallel with the activity of Cdk1, TRAMM is phosphorylated as the cell enters mitotis and dephosphorylated as the cell enters anaphase in parallel with degradation of cyclin B-Cdk1 (Milev et al., 2015). TRAMM also contains the Cdk1 consensus motif in 3 out of its 5 predicted phosphorylation sites. Moreover, per Phosphokinase 3.1 kinase prediction, Cdk1 was one of the possible kinases at site 182 with $p>0.5$. For confirming that Cdk1 is the kinase responsible for phosphorylating TRAMM, purified Cdk1 was incubated with recombinant purified TRAMM in the presence of ATP (without the use of radioactive labeling). TRAMM's molecular weight is expected to shift in the presence Cdk1 due to phosphorylation. Inconclusive results were obtained as western blots showed that TRAMM's molecular weight was identical in the presence and absence of Cdk1(results not shown). For future work, this experiment could be repeated by incubating purified Cdk1 with purified TRAMM in the presence of gamma labeled ATP to produce a clear and consistent result where TRAMM is expected to be radiolabeled.

TRAMM is among various proteins such as Aurora B and BubR1 which affect CENP-E localization to the kinetochores (Liu et al., 2007; Putkey et al., 2002). It is noteworthy that when compared to other proteins, TRAMM has the most dramatic effect on the localization of CENP-E. CENP-E and TRAMM co-localize early in mitosis when TRAMM is maximally phosphorylated. Upon depletion of CENP-E, some chromosomes are improperly attached to the microtubules and are incapable of aligning at the metaphase plate (Milev et al., 2015). This resembles the phenotype of TRAMM depletion (Yao et al., 2000), suggesting that there is a strong link between CENP-E and TRAMM. This link was further confirmed by a yeast two-hybrid interaction that clearly suggests that the two interact in vitro (Milev et al., 2015). Further investigation in this study showed that the two do not only interact in vitro but also associate in vivo. However, this result was irreproducible, which could be due to the weak and transient association between CENP-E and TRAMM. Further investigation is needed to confirm this interaction in vivo. This could include epitope tagging of TRAMM and creating a stable cell line expressing the tagged form of TRAMM. Precipitating TRAMM in mitotically arrested cells and using mass spectrometry or western blot would confirm whether CENP-E is among the interactors.

Here we aimed to analyze TRAMM in terms of structure and its newly reported function

in mitosis. Upon analyzing the secondary structure by bioinformatics, the presence of 4 TPR motifs in the C-terminal portion of the protein was identified. Since this motif is involved in protein-protein interactions, it is tempting to speculate that this domain binds to CENP-E. In addition, the amino-terminal portion of the protein is predicted to be mainly unstructured. This same region contains the 5 residues involved in phosphorylation.

In the absence of a structure for TRAMM, the understanding of the mechanism of its function is limited. To overcome this issue, efforts were made towards producing a protein suitable for structural studies. I purified the recombinant form of TRAMM by expressing it in Arctic Express cells. Arctic Express cells possess Cpn10 and Cpn60 chaperonins that could help fold the protein of interest at cold temperatures. As such, this allowed recombinant TRAMM to be expressed as a soluble protein, a necessary first step in any structural study. To determine the importance of the unstructured N-terminal region on both the nature and structure of TRAMM, a truncated construct of TRAMM (missing the N-terminal unstructured domain) was expressed in Arctic Express cells (results not shown). TRAMM was expressed in a soluble form, but was not eluting from the column, suggesting that the solubility of TRAMM was affected. This is consistent with unpublished results showing that truncated TRAMM at the N-terminal could not rescue and suppress TRAMM knockdown-induced mitotic arrest. Moreover, a phosphomimetic mutant that contained all five potential phosphorylation sites changed to aspartic acid residues was expressed in Arctic Express cells (results not shown). Once again, the solubility of TRAMM was altered and it was not eluting from the column despite its presence in both the total cell lysate and the supernatant. All together this could suggest that the folding of the unstructured N-terminal portion containing the phosphorylation sites could be altered during mitosis to help regulate the function of TRAMM.

The monodispersed purified TRAMM sample is a strong indicator of successful crystallization of TRAMM. To date, 6 mammalian TRAPP subunits (TRAPPC1-TRAPPC6) have been crystallized (Sacher et al., 2008). Revealing the three-dimensional structure of TRAMM will provide insights into its function and would allow us to address many unanswered questions. Despite the sequence homology, TRAMM could share similar folds with proteins that have known cell cycle related

functions that would give us more insights into TRAMM's mitotic function. Besides crystallography, the recombinant protein could be incubated with lysates from cells arrested either in interphase (to identify membrane trafficking interactors) or in mitosis (to identify cell division interactors of which we expect CENP-E). Once interactors are identified, truncated forms of TRAMM would be used to map the regions on TRAMM where these proteins interact.

Interestingly, ongoing research on several patients carrying mutations in TRAMM where the protein is undetectable results in a delay in mitosis (Milev et al, 2017). These patients have severe developmental delays, which could be correlated to the mitotic delay caused by the mutation in TRAMM. TRAMM is among many other proteins such as CHAMP1 (a zinc finger protein) that can cause defects in mitosis resulting in such diseases (Tanaka et al., 2016). It is noteworthy that one of the mutations identified in a patient with TRAMM mutations affects a highly conserved alanine that is a part of the TPR conserved motif (Zeytuni et al., 2012).

TRAMM is amongvarious TRAPP subunits that are involved in a wide range of cellular activities. For example, the TRAPP II complex has been implicated in Rabin8 centrosome targeting and cilia formation where C3, C9, and C10 are essential subunits for this process (Westlake et al., 2011).

Apart from its functions in the TRAPP complex, including membrane trafficking and cilia formation, TRAPPC9 is speculated to be a moonlighting protein that functions in the NF-kB pathway and neuronal differentiation in the cerebellum (Khattak et al., 2014). This is shown by TRAPPC9 interacting with NIK in a yeast two-hybrid screening, which is involved in the transcription of NF-kB. Mutations in TRAPPC9 have been identified in individuals that have microcephaly and non-syndromic autosomal-recessive mental retardation (Brunet and Sacher, 2014).

The TRAPPC4 protein was suggested to regulate ERK signaling, but it is still unclear whether this is done in a TRAPP context or not (Brunet and Sacher, 2014). In a yeast two hybrid screening, TRAPPC4 interacts with ERK2 and directly affects the levels of phospho-ERK1/2 due to the possible involvement in its transportation from the cytoplasm to the nucleus. This transportation mechanism may be a moonlighting

function as increased levels of TRAPPC4 and phosphor-ERK1/2 are present in the nucleus of colonic carcinoma tissues, which may be independent of the TRAPP complex (Zhao et al., 2011).

Other moonlighting functions involving the TRAPP complex are collagen secretion and glycosylation, which are specifically affected by TRAPPC2 and TRAPPC11 respectively (Jones et al., 2003; Venditti et al., 2012; DeRossi et al., 2016). TRAPPC2 mutations can be linked to skeletal specific X-linked Spondyloepiphyseal Dysplasia Tarda (SEDT) due to it altering collagen secretion and affecting Golgi integrity. The recruitment of TANGO1 (a collagen receptor) by TRAPPC2 leads to its interaction with Sar1 (GTP-bound COPII) that is critical to the dissociation of Sar1 from the membrane at ER exit sites (Venditti et al., 2012). Mutations in Sar1B have shown to cause defects in the dissociation of chylomicrons from the ER which may lead to various types of chylomicron retention diseases (CMRD) (Jones et al., 2003). Further research into the interactions of TRAPPC2 with this pathway may assist in better understanding chylomicron dissociation and unanswered questions around CMRD (Brunet and Sacher, 2014). Other subunits in the complex such as TRAPPC2L and TRAPPC11 have also shown to have affect Golgi fragmentation, and may cause disorders ranging from neurodevelopmental delay of newborn children to miscarriages and lethality (Wen et al., 2015; Sacher et al., 2014).

TRAPPC11 (a component of human TRAPP III) has shown to have critical effects on the Golgi and can be lethal to humans due to its high importance in development (Brunet and Sacher, 2014). One study has shown that the depletion of TRAPPC11 causes a stressed unfolded protein response (UPR), specifically ER stress-inducing UPR, which results in hypoglycosylation and accumulation of lipid droplets in fibroblasts (DeRossi et al, 2016). Viral insertion causing TRAPPC11 depletion in zebrafish was shown to reduce N-linked glycosylation which led to liver steatosis(DeRossi et al., 2016). In addition to the liver, TRAPPC11 plays a physiological role in multiple other tissues including the muscle, eye, brain, and bone (Liang et al., 2015). Although the detailed mechanisms causing the neurological and muscular defects in TRAPPC11 patients are still unknown, the vast majority of individuals with TRAPPC11 mutations suffer from intellectual disabilities and neuromuscular defects (such as type 2S limbe-girdle muscular dystrophy) caused by hypoglycosylation (Bögershausen et al., 2013). Collectively, the phenotype of TRAPPC11 patients clearly shows a wide TRAPPC11-opathy which could

be due to the impairment of TRAPPC11 functions in multiple processes.

Continual research on TRAPP and its subunits has shown its wide variety of moonlighting functions, which is found to play important roles in many cellular processes. This project has allowed us to take a step further to understand TRAMM and its newly reported function in mitosis. Yet many questions still need to be addressed, including: Is TRAMM a part of a multi-subunit complex during mitosis or does it only associate transiently with some protein partners such as CENP-E? Which phosphatase is responsible for dephosphorylating TRAMM? How does TRAMM associate back with the TRAPP complex during interphase? Not only the research in TRAMM and its correlation to the cell cycle needs further investigation, but research into the mammalian TRAPP complex as a whole is still in its infancy. The more we learn about the mammalian TRAPP complex, the greater we emphasize the importance of its research to better understand the cell's various functions including membrane trafficking and cell division.

Chapter 5: References

1. Abreu Velez AM, Howard MS. Tumor-suppressor Genes, Cell Cycle Regulatory Checkpoints, and the Skin. North American Journal of Medical Sciences 2015;7(5).
2. Aslam Khattak N, Mir A. Computational analysis of TRAPPC9: candidate gene for autosomal recessive non-syndromic mental retardation. CNS & Neurological Disorders-Drug Targets (Formerly Current Drug Targets-CNS & Neurological Disorders) 2014;13(4):699-711.
3. Barr FA, Elliott PR, Gruneberg U. Protein phosphatases and the regulation of mitosis. Journal of Cell Science 2011;124(14):2323.
4. Barrière C, Santamaría D, Cerqueira A, Galán J, Martín A, Ortega S, Malumbres M, Dubus P, Barbacid M. Mice thrive without Cdk4 and Cdk2. Molecular Oncology 2007;1(1):72-83.
5. Bassik Michael C, Kampmann M, Lebbink Robert J, Wang S, Hein Marco Y, Poser I, Weibezahn J, Horlbeck Max A, Chen S, Mann M, Hyman Anthony A, LeProust Emily M, McManus Michael T, Weissman Jonathan S. A Systematic Mammalian Genetic Interaction Map Reveals Pathways Underlying Ricin Susceptibility. Cell 2013;152(4):909-922.
6. Behrends C, Sowa ME, Gygi SP, Harper JW. Network organization of the human autophagy system. Nature 2010;466(7302):68-76.
7. Blatch GL, Lässle M. The tetratricopeptide repeat: a structural motif mediating protein-protein interactions. Bioessays 1999;21(11):932-939.
8. Bögershausen N, Shahrzad N, Chong Jessica X, von Kleist-Retzow J-C, Stanga D, Li Y, Bernier Francois P, Loucks Catrina M, Wirth R, Puffenberger Eric G, Hegele Robert A, Schreml J, Lapointe G, Keupp K, Brett Christopher L, et al. Recessive TRAPPC11 Mutations Cause a Disease Spectrum of Limb Girdle Muscular Dystrophy and Myopathy with Movement Disorder and Intellectual Disability. The American Journal of Human Genetics 2013;93(1):181-190.
9. Bonifacino JS, Glick BS. The Mechanisms of Vesicle Budding and Fusion. Cell 2004;116(2):153-166.
10. Brunet S, Sacher M. In Sickness and in Health: The Role of TRAPP and Associated Proteins in Disease. Traffic 2014;15(8):803-818.

11. Bucciarelli E, Giansanti MG, Bonaccorsi S, Gatti M. Spindle assembly and cytokinesis in the absence of chromosomes during Drosophila male meiosis. The Journal of Cell Biology 2003;160(7):993.

12. Caldas Gina V, DeLuca Jennifer G. Mad2 “Opens” Cdc20 for BubR1 Binding. Molecular Cell 2013;51(1):3-4.

13. Caldas GV, DeLuca KF, DeLuca JG. KNL1 facilitates phosphorylation of outer kinetochore proteins by promoting Aurora B kinase activity. The Journal of Cell Biology 2013.

14. Carmena M, Wheelock M, Funabiki H, Earnshaw WC. The Chromosomal Passenger Complex (CPC): From Easy Rider to the Godfather of Mitosis. Nature Reviews Molecular Cell Biology 2012;13(12):789-803.

15. Castedo M, Perfettini J, Roumier T, Kroemer G. Cyclin-dependent kinase-1: linking apoptosis to cell cycle and mitotic catastrophe. Cell Death and Differentiation 2002;9(12):1287.

16. Cheeseman IM, Desai A. Molecular architecture of the kinetochore-microtubule interface. Nature Reviews Molecular Cell Biology 2008;9(1):33-46.

17. De Souza CP, Osmani SA. Mitosis, not just open or closed. Eukaryotic Cell 2007;6(9):1521-1527.

18. Dephoure N, Zhou C, Villen J, Beausoleil SA, Bakalarski CE, Elledge SJ, Gygi SP. A quantitative atlas of mitotic phosphorylation. Proceedings of the National Academy of Sciences U S A 2008;105(31):10762-10767.

19. DeRossi C, Vacaru A, Rafiq R, Cinaroglu A, Imrie D, Nayar S, Baryshnikova A, Milev MP, Stanga D, Kadakia D. trappc11 is required for protein glycosylation in zebrafish and humans. Molecular Biology of the Cell 2016;27(8):1220-1234.

20. Dyson HJ, Wright PE. Intrinsically unstructured proteins and their functions. Nature Reviews Molecular Cell Biology 2005;6(3):197-208.

21. Errico A, Deshmukh K, Tanaka Y, Pozniakovsky A, Hunt T. Identification of substrates for cyclin dependent kinases. Advances in Enzyme Regulation 2010;50(1):375-399.

22. Foltz DR, Jansen LE, Black BE, Bailey AO, Yates JR, 3rd, Cleveland DW. The human CENP-A centromeric nucleosome-associated complex. Nature Cell Biology 2006;8(5):458-469.

23. Fu J, Bian M, Jiang Q, Zhang C. Roles of Aurora Kinases in Mitosis and Tumorigenesis. Molecular Cancer Research 2007;5(1):1.

24. Fung TK, Yam CH, Poon RYC. The N-terminal Regulatory Domain of Cyclin A Contains Redundant Ubiquitination Targeting Sequences and Acceptor Sites. Cell Cycle 2005;4(10):1411-1420.

25. Gavet O, Pines J. Activation of cyclin B1–Cdk1 synchronizes events in the nucleus and the cytoplasm at mitosis. The Journal of Cell Biology 2010;189(2):247.

26. Gavet O, Pines J. Progressive activation of CyclinB1-Cdk1 coordinates entry to mitosis. Developmental Cell 2010;18(4):533-543.

27. Godek KM, Kabeche L, Compton DA. Regulation of kinetochore–microtubule attachments through homeostatic control during mitosis. Nature Reviews Molecular Cell Biology 2015;16(1):57-64.

28. Godi A, Di Campli A, Konstantakopoulos A, Di Tullio G, Alessi DR, Kular GS, Daniele T, Marra P, Lucocq JM, De Matteis MA. FAPPs control Golgi-to-cell-surface membrane traffic by binding to ARF and PtdIns(4)P. Nature Cell Biology 2004;6(5):393-404.

29. Goh C-S, Lan N, Douglas SM, Wu B, Echols N, Smith A, Milburn D, Montelione GT, Zhao H, Gerstein M. Mining the Structural Genomics Pipeline: Identification of Protein Properties that Affect High-throughput Experimental Analysis. Journal of Molecular Biology 2004;336(1):115-130.

30. Grancell A, Sorger PK. Chromosome movement: Kinetochores motor along. Current Biology 1998;8(11):R382-R385.

31. Greener T, Zhao X, Nojima H, Eisenberg E, Greene LE. Role of cyclin G-associated kinase in uncoating clathrin-coated vesicles from non-neuronal cells. Journal of Biological Chemistry 2000;275(2):1365-1370.

32. Guo Y, Kim C, Ahmad S, Zhang J, Mao Y. CENP-E–dependent BubR1 autophosphorylation enhances chromosome alignment and the mitotic checkpoint. The Journal of Cell Biology 2012.

33. Howell BJ, McEwen BF, Canman JC, Hoffman DB, Farrar EM, Rieder CL, Salmon ED. Cytoplasmic dynein/dynactin drives kinetochore protein transport to the spindle poles and has a role in mitotic spindle checkpoint inactivation. The Journal of Cell Biology 2001;155(7):1159.

34. Hughes H, Stephens DJ. Assembly, organization, and function of the COPII coat. Histochemistry and Cell Biology 2008;129(2):129-151.

35. Ishikawa E, Ishikawa T, Morita YS, Toyonaga K, Yamada H, Takeuchi O, Kinoshita T, Akira S, Yoshikai Y, Yamasaki S. Direct recognition of the mycobacterial

glycolipid, trehalose dimycolate, by C-type lectin Mincle. The Journal of Experimental Medicine 2009;206(13):2879.

36. Jones B, Jones EL, Bonney SA, Patel HN, Mensenkamp AR, Eichenbaum-Voline S, Rudling M, Myrdal U, Annesi G, Naik S, Meadows N, Quattrone A, Islam SA, Naoumova RP, Angelin B, et al. Mutations in a Sar1 GTPase of COPII vesicles are associated with lipid absorption disorders. Nature Genetics 2003;34(1):29-31.

37. Kastan MB, Bartek J. Cell-cycle checkpoints and cancer. Nature 2004;432(7015):316-323.

38. Kettenbach AN, Schweppe DK, Faherty BK, Pechenick D, Pletnev AA, Gerber SA. Quantitative Phosphoproteomics Identifies Substrates and Functional Modules of Aurora and Polo-Like Kinase Activities in Mitotic Cells. Science Signaling 2011;4(179):10.1126/scisignal.2001497.

39. Kim JJ, Lipatova Z, Segev N. TRAPP Complexes in Secretion and Autophagy. Frontiers in Cell and Developmental Biology 2016;4:20.

40. Kim Y, Heuser JE, Waterman CM, Cleveland DW. CENP-E combines a slow, processive motor and a flexible coiled coil to produce an essential motile kinetochore tether. The Journal of Cell Biology 2008;181(3):411.

41. Kim Y-G, Raunser S, Munger C, Wagner J, Song Y-L, Cygler M, Walz T, Oh B-H, Sacher M. The Architecture of the Multisubunit TRAPP I Complex Suggests a Model for Vesicle Tethering. Cell 2006;127(4):817-830.

42. Lara-Gonzalez P, Westhorpe Frederick G, Taylor Stephen S. The Spindle Assembly Checkpoint. Current Biology 2012;22(22):R966-R980.

43. Lee K, Rhee K. PLK1 phosphorylation of pericentrin initiates centrosome maturation at the onset of mitosis. The Journal of Cell Biology 2011;195(7):1093.

44. Lee S-Y, Jang C, Lee K-A. Polo-Like Kinases (Plks), a Key Regulator of Cell Cycle and New Potential Target for Cancer Therapy. Development & Reproduction 2014;18(1):65-71.

45. Li Y, Gorbea C, Mahaffey D, Rechsteiner M, Benezra R. MAD2 associates with the cyclosome/anaphase-promoting complex and inhibits its activity. Proceedings of the National Academy of Sciences 1997;94(23):12431-12436.

46. Liang W-C, Zhu W, Mitsuhashi S, Noguchi S, Sacher M, Ogawa M, Shih H-H, Jong Y-J, Nishino I. Congenital muscular dystrophy with fatty liver and infantile-onset cataract caused by TRAPPC11 mutations: broadening of the phenotype. Skeletal Muscle 2015;5(1):29.

47. Lindqvist A. Cyclin B–Cdk1 activates its own pump to get into the nucleus. The Journal of Cell Biology 2010;189(2):197.
48. Lindqvist A, van Zon W, Karlsson Rosenthal C, Wolthuis RMF. Cyclin B1–Cdk1 Activation Continues after Centrosome Separation to Control Mitotic Progression. PLOS Biology 2007;5(5):e123.
49. Liu J-X, Srivastava R, Che P, Howell SH. An Endoplasmic Reticulum Stress Response in Arabidopsis Is Mediated by Proteolytic Processing and Nuclear Relocation of a Membrane-Associated Transcription Factor, bZIP28. The Plant Cell 2008;19(12):4111.
50. Lynch-Day MA, Klionsky DJ. The Cvt pathway as a model for selective autophagy. FEBS Letters 2010;584(7):1359-1366.
51. Mailand N, Podtelejnikov AV, Groth A, Mann M, Bartek J, Lukas J. Regulation of G(2)/M events by Cdc25A through phosphorylation-dependent modulation of its stability. The EMBO Journal 2002;21(21):5911-5920.
52. Malmanche N, Maia A, Sunkel CE. The spindle assembly checkpoint: Preventing chromosome mis-segregation during mitosis and meiosis. FEBS Letters 2006;580(12):2888-2895.
53. Malumbres M, Barbacid M. Cell cycle, CDKs and cancer: a changing paradigm. Nature Reviews Cancer 2009;9(3):153-166.
54. Mao Y, Desai A, Cleveland DW. Microtubule capture by CENP-E silences BubR1-dependent mitotic checkpoint signaling. The Journal of Cell Biology 2005;170(6):873.
55. Maro B, Howlett SK, Webb M. Non-spindle microtubule organizing centers in metaphase II-arrested mouse oocytes. The Journal of Cell Biology 1985;101(5):1665.
56. Marumoto T, Hirota T, Morisaki T, Kunitoku N, Zhang D, Ichikawa Y, Sasayama T, Kuninaka S, Mimori T, Tamaki N, Kimura M, Okano Y, Saya H. Roles of aurora-A kinase in mitotic entry and G2 checkpoint in mammalian cells. Genes to Cells 2002;7(11):1173-1182.
57. May KM, Hardwick KG. The spindle checkpoint. Journal of Cell Science 2006;119(20):4139.
58. Mayya V, Lundgren DH, Hwang S-I, Rezaul K, Wu L, Eng JK, Rodionov V, Han DK. Quantitative Phosphoproteomic Analysis of T Cell Receptor Signaling Reveals System-Wide Modulation of Protein-Protein Interactions. Science Signaling 2009;2(84):ra46.

59. McKinney-Freeman SL, Jackson KA, Camargo FD, Ferrari G, Mavilio F, Goodell MA. Muscle-derived hematopoietic stem cells are hematopoietic in origin. Proceedings of the National Academy of Sciences 2002;99(3):1341-1346.

60. Milev MP, Hasaj B, Saint-Dic D, Snounou S, Zhao Q, Sacher M. TRAMM/TrappC12 plays a role in chromosome congression, kinetochore stability, and CENP-E recruitment. The Journal of Cell Biology 2015;209(2):221.

61. Morgan DO. The cell cycle: principles of control: New Science Press; 2007.

62. Müller-Reichert T, Srayko M, Hyman A, O'Toole ET, McDonald K. Correlative Light and Electron Microscopy of Early Caenorhabditis elegans Embryos in Mitosis. Methods in Cell Biology 2007;79:101-119.

63. Musacchio A. Spindle assembly checkpoint: the third decade. Philosophical Transactions of the Royal Society B: Biological Sciences 2011;366(1584):3595.

64. Musacchio A, Salmon ED. The spindle-assembly checkpoint in space and time. Nature Reviews Molecular Cell Biology 2007;8(5):379-393.

65. Musinipally V, Howes S, Alushin GM, Nogales E. The Microtubule Binding Properties of CENP-E's C-Terminus and CENP-F. Journal of Molecular Biology 2013;425(22):4427-4441.

66. Nishi H, Hashimoto K, Panchenko Anna R. Phosphorylation in Protein-Protein Binding: Effect on Stability and Function. Structure 2011;19(12):1807-1815.

67. O'Connor C. Cell division: Stages of mitosis. Nature Education 2008;1(1):188.

68. Passmore LA, Barford D. Coactivator functions in a stoichiometric complex with anaphase-promoting complex/cyclosome to mediate substrate recognition. EMBO reports 2005;6(9):873-878.

69. Poduri A, Evrony GD, Cai X, Walsh CA. Somatic Mutation, Genomic Variation, and Neurological Disease. Science 2013;341(6141).

70. Potapova TA, Daum JR, Byrd KS, Gorbsky GJ. Fine Tuning the Cell Cycle: Activation of the Cdk1 Inhibitory Phosphorylation Pathway during Mitotic Exit. Molecular Biology of the Cell 2009;20(6):1737-1748.

71. Price Ii WN, Chen Y, Handelman SK, Neely H, Manor P, Karlin R, Nair R, Liu J, Baran M, Everett J, Tong SN, Forouhar F, Swaminathan SS, Acton T, Xiao R, et al. Understanding the physical properties that control protein crystallization by analysis of large-scale experimental data. Nature Biotechnology 2009;27(1):51-57.

72. Putkey FR, Cramer T, Morphew MK, Silk AD, Johnson RS, McIntosh JR, Cleveland DW. Unstable Kinetochore-Microtubule Capture and Chromosomal Instability Following Deletion of CENP-E. Developmental Cell 2002;3(3):351-365.

73. Royle SJ. The role of clathrin in mitotic spindle organisation. Journal of Cell Science 2012;125(1):19.

74. Royle SJ, Bright NA, Lagnado L. Clathrin is required for the function of the mitotic spindle. Nature 2005;434(7037):1152-1157.

75. Sacher M, Barrowman J, Wang W, Horecka J, Zhang Y, Pypaert M, Ferro-Novick S. TRAPP I Implicated in the Specificity of Tethering in ER-to-Golgi Transport. Molecular Cell 2001;7(2):433-442.

76. Sacher M, Jiang Y, Barrowman J, Scarpa A, Burston J, Zhang L, Schieltz D, Yates JR, Abeliovich H, Ferro-Novick S. TRAPP, a highly conserved novel complex on the cis-Golgi that mediates vesicle docking and fusion. The EMBO Journal 1998;17(9):2494-2503.

77. Sacher M, Kim Y-G, Lavie A, Oh B-H, Segev N. The TRAPP Complex: Insights into its Architecture and Function. Traffic 2008;9(12):2032-2042.

78. Sacher M, Milev M, Prematilake K, Larson A, Moore S, Koehler K, Huebner A, Jimenez-Mallabrera C. TRAPPC11 mutations lead to a diverse set of disorders with muscular dystrophy as a common feature. Molecular Biology of the Cell; 2016: AMER SOC CELL BIOLOGY 8120 WOODMONT AVE, STE 750, BETHESDA, MD 20814-2755 USA; 2016.

79. Salaun P, Rannou Y, Claude P. Cdk1, Plks, Auroras, and Neks: the mitotic bodyguards. Hormonal Carcinogenesis V: Springer; 2008. p. 41-56.

80. Santamaria D, Barriere C, Cerqueira A, Hunt S, Tardy C, Newton K, Caceres JF, Dubus P, Malumbres M, Barbacid M. Cdk1 is sufficient to drive the mammalian cell cycle. Nature 2007;448(7155):811-815.

81. Sardar HS, Luczak VG, Lopez MM, Lister BC, Gilbert SP. Mitotic Kinesin CENP-E Promotes Microtubule Plus-End Elongation. Current Biology 2010;20(18):1648-1653.

82. Satyanarayana A, Kaldis P. Mammalian cell-cycle regulation: several Cdks, numerous cyclins and diverse compensatory mechanisms. Oncogene 2009;28(33):2925-2939.

83. Scrivens PJ, Noueihed B, Shahrzad N, Hul S, Brunet S, Sacher M. C4orf41 and TTC-15 are mammalian TRAPP components with a role at an early stage in ER-to-Golgi trafficking. Molecular Biology of the Cell 2011;22(12):2083-2093.

84. Sivakumar S, Janczyk PŁ, Qu Q, Brautigam CA, Stukenberg PT, Yu H, Gorbsky GJ. The human SKA complex drives the metaphase-anaphase cell cycle transition by recruiting protein phosphatase 1 to kinetochores. Elife 2016;5:e12902.

85. Tanaka AJ, Cho MT, Retterer K, Jones JR, Nowak C, Douglas J, Jiang YH, McConkie-Rosell A, Schaefer GB, Kaylor J, Rahman OA, Telegrafi A, Friedman B, Douglas G, Monaghan KG, et al. De novo pathogenic variants in CHAMP1 are associated with global developmental delay, intellectual disability, and dysmorphic facial features. Cold Spring Harbor Molecular Case Study 2016;2(1):a000661.

86. Tang NH, Toda T. MAPping the Ndc80 loop in cancer: A possible link between Ndc80/Hec1 overproduction and cancer formation. BioEssays 2015;37(3):248-256.

87. Ubersax JA, Woodbury EL, Quang PN, Paraz M, Blethrow JD, Shah K, Shokat KM, Morgan DO. Targets of the cyclin-dependent kinase Cdk1. Nature 2003;425(6960):859-864.

88. Vader G, Medema RH, Lens SMA. The chromosomal passenger complex: guiding Aurora-B through mitosis. The Journal of Cell Biology 2006;173(6):833.

89. Velez AMA, Howard MS. Tumor-suppressor Genes, Cell Cycle Regulatory Checkpoints, and the Skin. North American Journal of Medical Sciences 2015;7(5):176-188.

90. Venditti R, Scanu T, Santoro M, Di Tullio G, Spaar A, Gaibisso R, Beznoussenko GV, Mironov AA, Mironov A, Zelante L, Piemontese MR, Notarangelo A, Malhotra V, Vertel BM, Wilson C, et al. Sedlin Controls the ER Export of Procollagen by Regulating the Sar1 Cycle. Science 2012;337(6102):1668.

91. Wang Q, Xie S, Chen J, Fukasawa K, Naik U, Traganos F, Darzynkiewicz Z, Jhanwar-Uniyal M, Dai W. Cell Cycle Arrest and Apoptosis Induced by Human Polo-Like Kinase 3 Is Mediated through Perturbation of Microtubule Integrity. Molecular and Cellular Biology 2002;22(10):3450-3459.

92. Weaver BAA, Bonday ZQ, Putkey FR, Kops GJPL, Silk AD, Cleveland DW. Centromere-associated protein-E is essential for the mammalian mitotic checkpoint to prevent aneuploidy due to single chromosome loss. The Journal of Cell Biology 2003;162(4):551.

93. Wen J, Hanna CW, Martell S, Leung PC, Lewis SM, Robinson WP, Stephenson MD, Rajcan-Separovic E. Functional consequences of copy number variants in miscarriage. Molecular Cytogenetics 2015;8(1):6.

94. Westlake CJ, Baye LM, Nachury MV, Wright KJ, Ervin KE, Phu L, Chalouni C, Beck JS, Kirkpatrick DS, Slusarski DC, Sheffield VC, Scheller RH, Jackson PK. Primary cilia membrane assembly is initiated by Rab11 and transport protein particle II (TRAPPII) complex-dependent trafficking of Rabin8 to the centrosome. Proceedings of the National Academy of Sciences 2011;108(7):2759-2764.

95. Yao X, Abrieu A, Zheng Y, Sullivan KF, Cleveland DW. CENP-E forms a link between attachment of spindle microtubules to kinetochores and the mitotic checkpoint. Nature Cell Biology 2000;2(8):484-491.

96. Zeytuni N, Zarivach R. Structural and Functional Discussion of the Tetra-Trico-Peptide Repeat, a Protein Interaction Module. Structure 2012;20(3):397-405.

97. Zhao S-L, Hong J, Xie Z-Q, Tang J-T, Su W-Y, Du W, Chen Y-X, Lu R, Sun D-F, Fang J-Y. TRAPPC4-ERK2 Interaction Activates ERK1/2, Modulates Its Nuclear Localization and Regulates Proliferation and Apoptosis of Colorectal Cancer Cells. PLOS ONE 2011;6(8):e23262.

98. Zong M, Wu X-g, Chan CWL, Choi MY, Chan HC, Tanner JA, Yu S. The Adaptor Function of TRAPPC2 in Mammalian TRAPPs Explains TRAPPC2-Associated SEDT and TRAPPC9-Associated Congenital Intellectual Disability. PLOS ONE 2011;6(8):e23350.